

Design of an Automated Guided Vehicle for Material Handling

Maria Margarida Malveiro Bento das Dores Cheira

Thesis to obtain the Master of Science Degree in
Aerospace Engineering

Supervisors: Prof. Filipe Szolnoky Ramos Pinto Cunha
Prof. Luís Filipe Galrão dos Reis

Examination Committee

Chairperson: Prof. Fernando José Parracho Lau
Supervisor: Prof. Filipe Szolnoky Ramos Pinto Cunha
Members of the Committee: Prof. Rosa Maria Marquito Marat Mendes
Eng. Fernando José Loureiro da Silva

July 2019

"However difficult life may seem, there is always something you can do and succeed at.

It matters that you don't just give up."

– Stephen Hawking

I declare that this document is an original work of my own authorship and that it fulfills all the requirements of the Code of Conduct and Good Practices of the Universidade de Lisboa.

Acknowledgments

The completion of this thesis would not have been possible if not for the help and support of a few individuals, to whom I would like to take the chance to express my gratitude.

I want to start by thanking my supervisors at IST, Professor Filipe Cunha and Professor Luis Reis, for their guidance and advice. I would also like to thank my supervisor at TAP, Engineer Fernando Loureiro, for his continuous support during my time at TAP.

The biggest thank you goes to my mom and dad. Thank you for being my #1 fans. Thank you for all the unconditional love, support, encouragement, patience, and for always believing that I am capable of anything. Thank you for allowing me to do this at my own pace.

To my big sister, whom I've always looked up to, thank you for being my idol and my role model. And above all, thank you for understanding my struggles and being the one person to assure me that the best is yet to come.

To my friends and former classmates, from this hopeless socially awkward person, I thank you just for giving me the gift of your friendship. Thank you for bringing some fun times to the stressful life that was being an IST student.

Finally, to Guilherme, my boyfriend and best friend, thank you for seeing me through the chaotic mess that has been this past year. Finishing my degree has posed a much bigger challenge than I had anticipated, more often than not bringing me down to my knees, and you've always been the helping hand to bring me back up on my feet. Thank you for listening to me constantly and pointlessly rant about my hardships and frustrations, and never ceasing to offer your support. Thank you for being my rock and for giving me a reason to keep going.

Resumo

Esta tese foca-se na conceptualização e *design* de um veículo guiado automaticamente (AGV) para transporte de material, para ser implementado numa oficina da TAP. Actualmente, o transporte de material é feito manualmente com o auxílio de carros de transporte de material.

Baseado num *design* preliminar feito previamente a esta tese e na actividade actual da oficina, foi esboçado um primeiro conceito de um AGV que rebocaria um carrinho. De seguida, foi feita uma análise dos carrinhos actuais, e foi desenvolvido um mecanismo de forma a permitir a distribuição autónoma do material, bem como sugeridas adaptações por forma a permitir o acoplamento entre o AGV e o carrinho.

As forças às quais o carrinho e o AGV estarão sujeitas foram então analisadas e calculadas a partir de valores assumidos para as dimensões do AGV. Estas permitiram o cálculo do torque necessário para o AGV puxar o carrinho, o que por sua vez permite o dimensionamento do motor. Também foi calculado se o AGV teria tracção suficiente de modo a puxar o carrinho sem escorregar, e foram testados alguns dos piores cenários possíveis de modo a discernir em que situações o AGV consegue ou não realizar a sua função.

Finalmente, foi realizada uma análise estrutural através de uma simulação computacional para prever se a estrutura do AGV conseguia cumprir com as especificações de *design*.

Palavras-chave: Manuseamento de materiais, Veículo guiado automaticamente, Resistência de rolemento, Design, Método de elementos finitos

Abstract

This thesis is focused on the conceptualization and design of an automated guided vehicle (AGV) for material handling, to be implemented at a workshop at TAP. The material handling is currently done manually with the aid of carts.

Based on a preliminary design done prior to this thesis and the current activity at the workshop, a first concept for a AGV that would tow the carts was drafted. Following this, an analysis of the current carts is done, and a mechanism is developed in order to allow the carts to distribute material autonomously, as well as adaptations are suggested in order to allow the AGV to attach to the carts.

The loads to which the AGV and the cart are subjected are then analysed and calculated by making assumptions about the dimensions of the AGV. These allow for the calculation of the torque required for the AGV to pull the cart, which then allows for the dimensioning of the motor. It is also verified whether the AGV has enough traction to be able to pull the cart without slipping, and a few worst case scenarios are tested to provide insight on what situations the AGV can and can not function.

Finally, a structural analysis is performed through a computational simulation to predict whether or not the structure of the AGV can withstand the loads previously calculated without yielding or disassembling.

Keywords: Material handling, Automated Guided Vehicle, Rolling resistance, Design, Finite element analysis

Contents

Acknowledgments	vii
Resumo	ix
Abstract	xi
List of Tables	xv
List of Figures	xvii
Nomenclature	xix
Glossary	xxi
1 Introduction	1
1.1 Motivation	1
1.2 Topic Overview - AGV History	2
1.3 TAP Air Portugal	3
1.4 Objectives	3
1.5 Thesis Outline	3
2 Theoretical Background	5
2.1 Kinetics of an Electric Vehicle	5
2.1.1 Rolling Resistance Force	5
2.1.2 Aerodynamic Drag	7
2.1.3 Force of Gravity on an Inclined Plane	8
2.1.4 Tractive Effort and relation with Torque	8
3 Project Framework	11
3.1 Continuous Improvement	11
3.1.1 Kaizen Philosophy	11
3.2 Workspace and Current Activity	12
3.3 Requirements and Constraints	14
3.4 Previous Work	14
3.4.1 Guide Path Configuration and Navigation	15
3.4.2 Vehicle Type and Wheel Configuration	16
3.4.3 Battery Type and Charging Scheme	17
3.4.4 Fleet Size	18

3.4.5 Safety Devices	18
3.4.6 Preliminary Design	19
4 Material Distribution System	21
4.1 Analysis of the Preliminary Design and Concept Adaptations	21
4.2 Cart Adaptations	22
4.2.1 Current Carts and Cargo	22
4.2.2 Distribution System	24
4.2.3 Expedition System	29
4.2.4 Coupling	30
4.2.5 Final Cart Design	32
4.3 Designing the AGV	32
4.3.1 First Considerations	32
4.3.2 Equations of Motion	33
4.3.3 First Design Iteration	34
4.3.4 3D sketch of the AGV	38
4.3.5 Second Design Iteration	38
4.3.6 Further design considerations	41
5 Structural Analysis	43
5.1 Material Properties	43
5.2 Finite Element Analysis	46
5.2.1 Finite Element Method	46
5.2.2 Meshing	46
5.2.3 Modelling the geometry	47
5.2.4 Loads and Constraints	48
5.2.5 Linear Static Analysis	48
6 Conclusions	51
6.1 Future Work	51
Bibliography	53
A C.F.R. Drive Wheel Technical Datasheet	57
B AGV Dimensions and Structure	59

List of Tables

3.1 AXX4-8/6 P Lifting Table information	17
3.2 Steerable drive wheel information	17
3.3 U1-24RT characteristics	18
3.4 S3000 standard safety laser scanner information	18
3.5 Components information	19
3.6 Vehicle total dimensions	19
4.1 Empirical values for rolling resistance coefficient [34]	36
4.2 First iteration results	36
4.3 New steerable drive wheel information	37
4.4 Lithium Ion battery 12V 70Ah – LiFePO4 – PowerBrick specifications	37
4.5 Second iteration results	39
4.6 Attributes of Polyurethane and Rubber [36]	40
4.7 Jammed wheels with cart in movement	40
4.8 Jammed wheels with cart in resting state	41
5.1 Deflection in mm for a T1 tube suspending a central load	44
5.2 Deflection in mm for a T2 tube suspending a central load	44
5.3 Young's modulus in GPa for T1	45
5.4 Young's modulus in GPa for T2	45
5.5 Mechanical properties for E260 steel	45
5.6 FEA results	49

List of Figures

1.1	Number of publications with the phrase "Automated Guided Vehicle" through time [4]	2
2.1	Forces acting on a moving vehicle (front wheel drive).	5
2.2	Forces acting on a wheel being pulled (adapted from [8]). The normal reaction is the result of the uneven distributed force.	6
2.3	Force of gravity on a vehicle moving uphill.	8
2.4	Free body diagram of a motorized wheel.	9
3.1	Partial plant of the workshop. Areas outlined in black represent the four work groups, and in blue is the reception/expedition area. Some dimensions (meters) were highlighted for scale.	12
3.2	Reception/Expedition Area	13
3.3	Colourful trays	13
3.4	Cart with trays	13
3.5	Expedition shelves	13
3.6	Magnetic tape and sensor [17]	15
3.7	Single loop path with a single unidirectional lane [5]	16
3.8	Example of an underride AGV carrying a cart [18]	16
3.9	HYMO AXX4-8/6 P Lifting Table [19]	16
3.10	Tricycle configuration (adapted from [20])	17
3.11	C.F.R. Steerable drive wheel [21]	17
3.12	Preliminary design of the AGV (adapted from [5])	20
4.1	Cart dimensions in mm	22
4.2	Back view of the cart	22
4.3	Connectors [22]	23
4.4	Intermediate support type connector [22]	24
4.5	Tray delivery. Cart is represented in black and reception shelf is represented in green	25
4.6	Pictures and schematics of the mechanism [28]	25
4.7	Pictures and schematics of the mechanism [28]	26
4.8	Solution provided by Quimilock	26
4.9	Locking mechanism	27

4.10 Rotating connector (image from [22])	27
4.11 Roller wheel schematics (adapted from [29])	27
4.12 Rollers at different heights (adapted from [28])	27
4.13 Adjustable rollers (adapted from [28])	28
4.14 Vertical misalignment (adapted from [28])	28
4.15 Schematic view from above. The reception shelves are represented in green, the ramps in grey, the rollers in blue, and the offset in yellow. The arrow represents the direction of motion of the cart	29
4.16 Horizontal misalignment. The yellow shaded areas represent the rollers and ramps that have an offset, and the arrow represents the direction of motion of the cart	29
4.17 Example of mechanism for expedition shelves	30
4.18 Coupling structure (sectioned view)	31
4.19 Castor with tube plug-in pin [31]	31
4.20 3D drawings of the cart (dimensions in mm)	32
4.21 Free body diagrams	33
4.22 3D drawings of the AGV	38
4.23 Weight distribution on AGV	39
4.24 Contact charging system [37]	41
4.25 Contactless charging system [39]	42
 5.1 Tube sections (lighter grey represents the coating while the darker grey represents the steel)	43
5.2 Simply supported beam with central load [42]	44
5.3 Joint strength (Adapted from [41])	45
5.4 Modelling of the AGV	47
5.5 Loads and constraints	48
5.6 Mesh convergence study	49
5.7 Displacement – Magnitude	50
5.8 von Mises Stress	50
5.9 Shear Force XY	50
5.10 Shear Force XZ	50
5.11 Axial Force	50
 B.1 AGV dimensions, side	59
B.2 AGV dimensions, top	59
B.3 AGV structure	60
B.4 AGV structure detail	60

Nomenclature

Greek symbols

α	Angular acceleration.
μ	Dynamic viscosity.
μ_k	Kinetic friction coefficient.
μ_s	Static friction coefficient.
μ_{rr}	Rolling friction coefficient.
ν	Kinematic viscosity.
ω	Angular velocity.
ρ	Density.

Roman symbols

A	Area.
a	Acceleration.
C_D	Drag coefficient.
C_f	Skin friction drag coefficient.
C_p	Pressure drag coefficient.
E	Young's modulus.
F	Force.
g	Gravity.
h	Fraction of dissipated energy.
I	Moment of inertia.
J	Second moment of area.
L	Length.

M Moment.

m Mass.

P Vertical load.

p Power.

R Normal reaction.

r radius.

Re Reynold number.

s Width of wheel.

T Torque.

t Thickness.

V Volume.

v Speed.

W Weight.

Subscripts

rr Rolling resistance.

x, y Cartesian components.

Glossary

- AGV** Automated Guided Vehicle is a vehicle that doesn't rely on a human driver.
- FEA** Finite element analysis is a computational analysis that uses the finite element method.
- FEM** Finite element method is a numerical method of solving differential equations by dividing the domain into several elements.
- HP** Hydraulic and pneumatic.
- M&E** Maintenance & Engineering.
- RE** Reception and expedition.

Chapter 1

Introduction

1.1 Motivation

The high demands of an increasingly competitive market, along with the fast rhythm at which technological advancements are achieved nowadays, are leading many companies to adopt strategies to optimize their processes and upgrade the quality of their products, as well as making continuous efforts to adjust and improve their production systems in order to not fall behind.

When talking about the tasks of intralogistics in industrial environments, material handling appears as one the most important tasks, as it heavily impacts the flow of material and, consequently, the efficiency of the production process and its potential profitability [1].

For many years, the classical method used by companies was manual material handling, where the material was transported manually by workers. Nowadays, the increasing trend has been the automation of these tasks through the use of Automated Guided Vehicles (AGV). An AGV, as the name might imply, is a vehicle that doesn't rely on a human driver.

One of the most famous examples of a company using this type of solution is Amazon, which in 2012 bought a robotics company for \$775 million with the sole intention of using their robots internally to improve logistics efficiency within their fulfilment centers. Amazon now has over 45 thousand robots across 20 fulfilment centers [2].

While replacing a human with a robot might have some drawbacks, namely the decreased flexibility and the high initial investment, it also has many advantages. AGVs don't require salaries or promotions, reducing labour costs. They can work in conditions that could be potentially compromising to human safety, and, even though they are usually equipped with safety sensors, in case of an accident the AGV doesn't become injured, improving safety conditions in the workspace. Finally, the AGV doesn't become tired, doesn't require resting time, doesn't require vacation, and doesn't become distracted, contributing to increased productivity and accuracy [3].

1.2 Topic Overview - AGV History

The history of the AGV begins in 1953 with the creation of the first one. The AGV was first invented in the U.S.A. by Arthur Barret, Jr., who made adaptations to a man-driven tow truck so that it would follow a wire in the ceiling. He named his invention the "Guide-O-Matic" and described it as a "driverless vehicle". His company, Barret Electronics, was the first ever to implement and commercialize this idea. The company is nowadays known as Savant Automation and still specializes in the supply of AGV systems. By the time the idea was first commercialized, the AGV had already evolved into following a wire embedded on the floor. Not long after, other versions of this machine started being marketed in Europe as well, some of them used optical sensors to follow coloured strips on the floor. The AGVs of this first era were marked by their simple functioning. They followed a specific path in a single direction and relied on bumpers equipped with tactile sensors for safety [1].

The years from the 1970s to the early 1990s saw the appearance of high-performance electronics, microprocessors, and programmable logic controllers (PLC), which improved the precision in navigation and allowed for more complex use scenarios, batteries grew more powerful, and infrared and radio signals were used for data transfer. In the late 80s a severe recession hit the industry. Around the same time, the concept of Lean Production, which promised a simple way to improve quality while reducing manufacturing costs, began to spread. At this time, AGVs were known to be big and expensive machines, and, combining that with their limited flexibility, made them less desirable, marking the dawn of this era and the beginning of a new one [1].

From the late 90s to the 2010s, AGVs evolved into much more sophisticated, reliable, and flexible machines. Improved sensory technology allowed for faster vehicles. They were now controlled by standard PCs, and new navigation technologies allowed for the AGVs to navigate freely and for better manoeuvrability. WLAN also established itself as a means of data transfer [1]. Up until this point, the AGV was mostly used in factories and warehouses, but it has since expanded into numerous other industries, including hospitals.

Overall, the AGV has been an ever increasing trend, as made obvious by Figure 1.1, which shows the number of publications with the phrase "Automated Guided Vehicle" in its title, abstract or keywords from the first digital publications in 1974 and up to 2016.

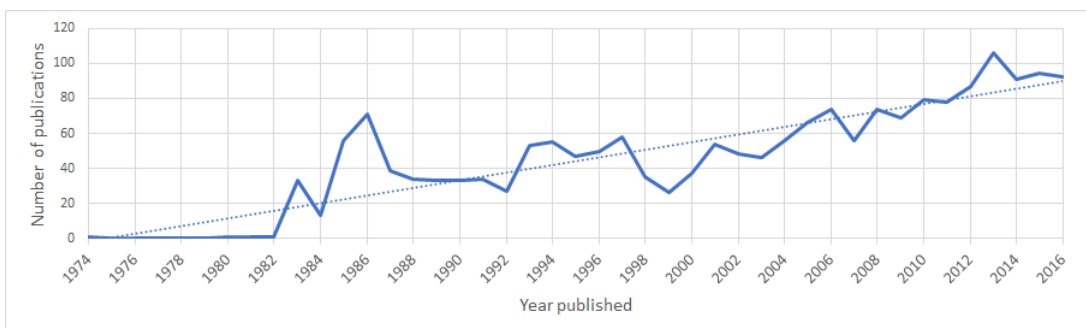


Figure 1.1: Number of publications with the phrase "Automated Guided Vehicle" through time [4]

1.3 TAP Air Portugal

TAP Air Portugal, commonly referred to as just TAP, is the Portuguese flag carrier airline, having its headquarters in Lisbon and its main hub at the Lisbon Airport.

TAP was founded in 1945, its first fleet composed of two DC-3 Dakota, and its first commercial flight in 1946 flew 11 passengers plus crew from Lisbon to Madrid. Now, TAP flies to over 90 destinations and counts on a fleet of over 90 aircraft, and, in 2018, flew 16 million passengers.

This project was developed within the department of Continuous Improvement of the TAP Maintenance & Engineering (M&E) division.

1.4 Objectives

The purpose of this thesis is to design an AGV to be introduced at the hydraulic and pneumatic (HP) workshop at TAP M&E and used for material handling.

An analysis will be made of the preliminary design made by Enrique Martínez [5] and adaptations will be suggested. The design will then be constructed based on the conclusions of Martínez's thesis [5] and the suggested adaptations. Calculations and a structural analysis should be performed in order to ensure the design works and is structurally sound.

1.5 Thesis Outline

This thesis is divided into six chapters:

- Chapter 1 presents the motivation for this thesis, a little bit of history of the subject, and defines the main objectives.
- Chapter 2 outlines the theory behind the kinetics of an electric vehicle and enumerates some of the main equations required for this project.
- Chapter 3 provides the context for this project, giving a little bit of insight about the department within which this thesis was developed and the workshop where this project is going to be applied to, as well as the work that has been previously done on this subject.
- Chapter 4 details all the steps taken in coming up with a design for the material distribution system. It begins with an analysis of the conclusions taken in previous work, and moves on to detail the reasoning behind the design choices that were made, as well as some calculations to back up the validity of the design.
- Chapter 5 includes a structural analysis of the design achieved in the previous chapter to understand if the structure can support the loads to which it will be subjected.
- Chapter 6 summarizes the achievements of this project and provides suggestions for additional work that could be done on this subject in the future.

Chapter 2

Theoretical Background

2.1 Kinetics of an Electric Vehicle

In order to begin modelling an electric vehicle, it's important to understand the relationship between the motion the vehicle is required to generate and the forces that it will be subjected to. An equation, or a system of equations, must then be produced in order to fully define the vehicles motion.

The typical forces a vehicle will usually have to overcome are the rolling resistance (F_{rr}), the aerodynamic drag (F_{ad}), the component of the weight (W) that is parallel to the ground (F_{slope}) in case there is a slope, as well as any other external forces that may be acting on the vehicle (F_{ext}). The force that will propel the vehicle forward is typically called the tractive effort (F_{te}) [6]. All these forces can be seen represented in Figure 2.1.

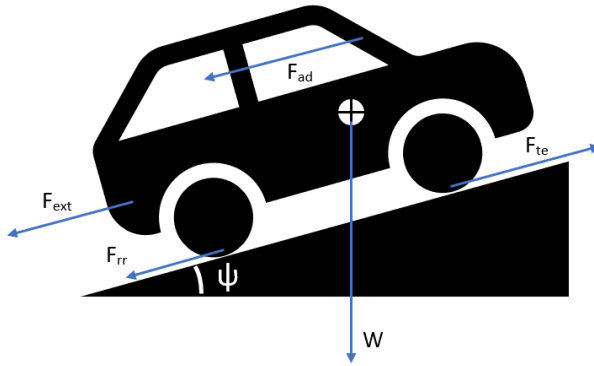


Figure 2.1: Forces acting on a moving vehicle (front wheel drive).

2.1.1 Rolling Resistance Force

Rolling resistance exists due to the fact that under a vertical load, even if it's just the weight of the wheel, the wheel and the ground will deform slightly, and the contact between the wheel and the ground will take place over an area rather than a point [7]. Because the material of the wheel isn't perfectly elastic, as the wheel turns and the material is compressed and released there will be energy losses. Translating this to forces, it means that the force distribution in the contact area will not be even [8]. As

such, the resulting upwards force, the normal reaction, will be misaligned with the centre of the wheel, as can be seen in Figure 2.2.

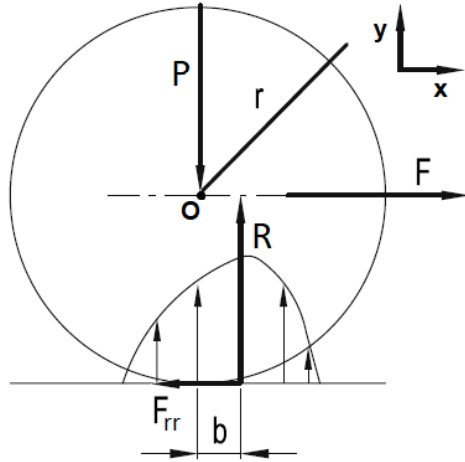


Figure 2.2: Forces acting on a wheel being pulled (adapted from [8]). The normal reaction is the result of the uneven distributed force.

Applying the dynamic equations of motion results:

$$\sum F_x = m_{wheel}a = F - F_{rr} \quad (2.1)$$

$$\sum F_y = 0 = R - P \Leftrightarrow R = P \quad (2.2)$$

$$\sum M_0 = I\alpha = I \frac{a}{r} = F_{rr}r - Rb \Leftrightarrow F_{rr} = I \frac{a}{r^2} + \mu_{rr}R \quad (2.3)$$

where m_{wheel} = mass of the wheel

a = acceleration

r = radius of the wheel

b = horizontal distance between R and the centre of the wheel

P = total vertical load on the wheel (including weight)

R = normal reaction

F = force pulling the wheel

F_{rr} = rolling resistance

I = moment of inertia of the wheel

$\alpha = \frac{a}{r}$ = angular acceleration of the wheel

$\mu_{rr} = \frac{b}{r}$ = rolling friction coefficient

The rolling friction coefficient, μ_{rr} , is usually determined through experimental tests, seeing as it depends on parameters such as load, speed, type of tyre, terrain, etc., in a way that has not yet been well established [7].

2.1.2 Aerodynamic Drag

Drag is the force that a fluid will exert on a moving body that is opposite to its relative motion. Aerodynamic drag is the term used when the surrounding fluid is air, and it can be expressed by the following equation:

$$F_{ad} = \frac{1}{2}\rho_{air}v^2C_D A \quad (2.4)$$

where ρ_{air} = air density

v = relative speed between fluid and body

C_D = drag coefficient

A = characteristic area

The characteristic area can be one of three types, depending on the type of body [9]:

1. Frontal area: the body as seen from the perspective of the stream (suitable for stubby bodies such as spheres, cylinders, cars).
2. Planform area: the body as seen from above (suitable for flat and wide bodies such as flat plates and wings).
3. Wetted area: the area of the body in contact with the flow, or immersed in the fluid (typically used in maritime and aeronautical applications).

As for the drag coefficient, C_D , it can be divided into two components, which are the pressure drag coefficient, C_p , and the skin friction drag coefficient, C_f (Equation 2.5) [9, 10]. The pressure drag relates to the pressure distribution around the body, meaning it's dependent on the shape of the body. The skin friction drag, on the other hand, is related with the viscosity of the fluid and varies with the Reynolds number, Re , which is the ratio between inertial force and viscous force (Equation 2.6) [10].

$$C_D = f(shape, Re) = C_p + C_f \quad (2.5)$$

$$Re = \frac{\rho v L}{\mu} = \frac{v L}{\nu} \quad (2.6)$$

where μ = dynamic viscosity of the fluid

ν = kinematic viscosity of the fluid

L = characteristic length

It is also usual to hear about lift induced drag and wave drag. However, those relate to bodies that generate lift and bodies moving at transonic/supersonic speeds, respectively. Since that is not the case with this project, those components will be ignored.

2.1.3 Force of Gravity on an Inclined Plane

When a vehicle is moving in an inclined plane, the force of gravity is naturally going to have a component that is normal to the ground and another that is parallel. This situation is represented in Figure 2.3, using the example from Figure 2.1.

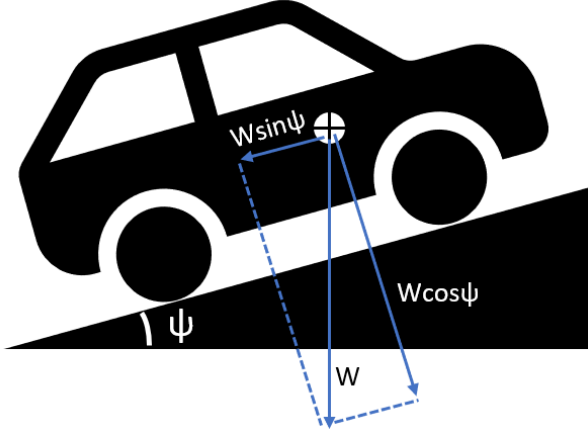


Figure 2.3: Force of gravity on a vehicle moving uphill.

As can be seen, only the component parallel to the ground will oppose the movement, so this resistance force can be defined as:

$$F_{slope} = W \sin\psi \quad (2.7)$$

2.1.4 Ttractive Effort and relation with Torque

As mentioned earlier, tractive effort is the force that propels the vehicle forward, and must be able to overcome all the forces that were described above, as well as any external forces that may be acting on the vehicle. As such, the tractive effort can be defined by equation 2.8, where x is the direction of motion, $m_{vehicle}$ is the mass of the vehicle, and $F_{ext,x}$ is the x component of the external forces.

$$\sum F_x = m_{vehicle}a \Leftrightarrow F_{te} = m_{vehicle}a + F_{rr} + F_{ad} + F_{slope} + \sum F_{ext,x} \quad (2.8)$$

Note that F_{slope} should be negative if the vehicle is going downhill.

This force is the result of the static friction that occurs between the wheel and the ground as a result from a torque being applied to the wheel by a motor. The free body diagram of a motorized wheel pulling a load can be seen in Figure 2.4.

Applying the dynamic equations of motion results:

$$\sum F_x = m_{wheel}a = F_{te} - F_r \Leftrightarrow F_r = F_{te} - m_{wheel}a \quad (2.9)$$

$$\sum F_y = 0 = R - P \Leftrightarrow R = P \quad (2.10)$$

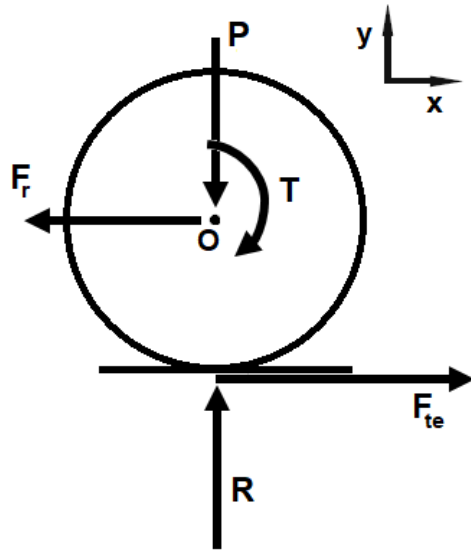


Figure 2.4: Free body diagram of a motorized wheel.

$$\sum M_0 = I\alpha = I \frac{a}{r} = T - F_{te}r \Leftrightarrow T = F_{te}r + I \frac{a}{r} \quad (2.11)$$

where F_r = load being pulled

T = torque

It's also worth noting that the torque a motor outputs is directly related to the power it draws [11].

$$T = \frac{p}{\omega} \quad (2.12)$$

where p is the power and ω is the angular velocity.

Chapter 3

Project Framework

3.1 Continuous Improvement

As mentioned previously, this project was developed within the Continuous Improvement ("Melhoria Contínua") department at TAP M&E.

The continuous improvement process, as the name might indicate, consists on a continuous and systematic effort to improve the effectiveness and efficiency of processes or services. It is greatly based on the Kaizen philosophy.

3.1.1 Kaizen Philosophy

"Kaizen" is a Japanese word that derives from the words "Kai", which means "change", and "Zen", which means "better" [12]. So "Kaizen" can be translated to "change for the better" or simply "improve". Masaaki Imai, who is considered to be the father of Continuous Improvement and is the founder of the Kaizen Institute, was the first to introduce the concept in the West, in 1986, through his book "Kaizen: The Key to Japan's Competitive Success" [13]. This philosophy is based on the idea that everything can be improved in order to perform better or more efficiently, and one of its great principles is that the build-up of small changes, rather than big, revolutionizing ones, are easier and quicker to implement, and shall lead to ever improving processes. Another big principle of the Kaizen philosophy is that the responsibility of making improvements within a company or organization falls on every one of its workers, from the highest to the lowest positions [14, 15].

One of the goals behind continuous improvement is to identify and minimize, or even eliminate, anything that can be considered wasteful. This is typically referred to as Lean production [16]. Usually, waste is defined as anything that doesn't add value to the process, which, from a monetary point of view, can be seen as any part of a process that represents a cost for the company but that won't add value to the final product, which is to say, the customer won't pay for it.

There are seven types of waste that are typically defined:

- **Overproduction:** When production is done faster, sooner or in larger quantities than what is

strictly necessary.

- **Transportation:** Time spent moving around material, parts, tools, or even people, to where they are needed is considered waste. Objects and people that are needed for a certain activity should be kept close to it to minimize the need for constant transportation.
- **Inventory:** Inventory should ideally be kept at the minimum needed to keep a process going. Any amount above that is considered waste.
- **Wait:** Time spent in inactivity waiting for something necessary to complete a task.
- **Over-Processing:** Any work done which is redundant or excessive.
- **Re-Processing:** Any work done which is not up to standard and needs to be redone.
- **Motion:** Not to be confused with transportation, motion refers to any type of movement done which does not add value to the task.

Some sources add an extra item to this list:

- **Talent:** When a certain activity is performed by someone who is overqualified or is more qualified to perform a different type activity.

It's important to note that most times it's impossible to completely eliminate waste, and that the goal is usually to optimize tasks by minimizing the waste.

3.2 Workspace and Current Activity

The AGV being developed in this thesis is meant to be introduced in the HP workshop at TAP. This workshop is divided into several groups, each dedicated to a different category of part or type of repair. Due to constraints regarding the layout of the workshop, this thesis will be focused on only four main groups, two on each side of a 5 meter wide corridor, as can be seen on Figure 3.1.

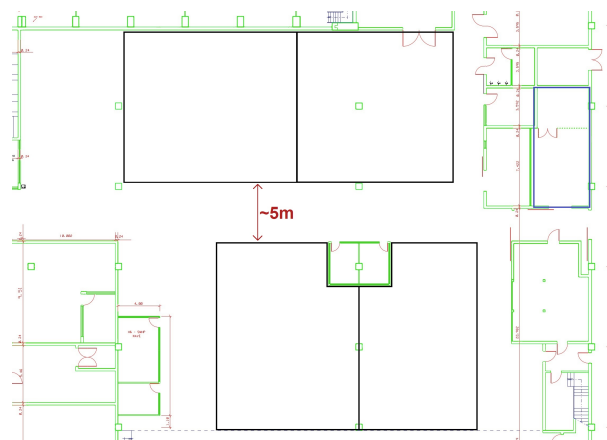


Figure 3.1: Partial plant of the workshop. Areas outlined in black represent the four work groups, and in blue is the reception/expedition area. Some dimensions (meters) were highlighted for scale.

Each day, parts are delivered at the reception/expedition (RE) area in need of repair or maintenance. There, workers separate the parts into trays according to which group they are meant to be delivered to. To each group is assigned a specific coloured tray, so that during the distribution it's easy to identify which trays go to each group. There are three sizes of trays, 600x400 mm, 400x300 mm, and 300x200 mm. Each part or set of parts is put into a tray as small as they can reasonably fit.



Figure 3.2: Reception/Expedition Area



Figure 3.3: Colourful trays

A worker will then deliver the trays with the aid of a cart. In each group there are two separate but similar stations containing shelves: an expedition station and a reception station. The worker places the trays with the unrepairs parts in the reception station and takes the trays with the repaired parts from the expedition station. After repeating this process for the other groups, the worker returns to the RE area with the trays containing the repaired parts.



Figure 3.4: Cart with trays



Figure 3.5: Expedition shelves

These pick-up and delivery tasks are done based on a concept called *Mizusumashi*, which consists on defined routes, which start and finish on the same location, have defined stop points, and defined schedules. The routes are also usually high frequency as to carry less cargo in each run.

There are five different routes and three people with three different schedules who each split their

time between performing some of these routes and other activities. Between the three workers there are twenty half-hour shifts dedicated to these routes, which equates to 10 hours per day dedicated to transporting material. It is worth to note that these routes include other areas besides the four that this thesis focuses on, so the AGV is not expected to work 10 hours a day, considering the current activity of the workshop.

It's obvious that these tasks require both transportation and motion, which, as mentioned previously in Section 3.1.1, are considered forms of waste, seeing as TAP needs to pay workers to perform these tasks, but, in the end, the time spent on them doesn't add value to the final product, and, as such, it's not something the client is interested in paying for. To a smaller extent, these tasks also constitute some waste of talent, seeing as they don't require any kind of special skill.

With the introduction of the AGV, the tasks described earlier should remain mostly the same, except they will be performed by the AGV instead of workers. As such, the waste associated with transportation will remain the same. However, the waste associated with motion will be largely reduced, as workers won't need to follow along the material being transported. This will result in a lot of extra time for the workers to focus on other tasks and increase productivity.

3.3 Requirements and Constraints

In order to design the AGV, some requirements had to be outlined. In terms of more general requirements, the idea behind the AGV is that it must be able to follow a defined path, know when to stop, and be able to recognize obstacles and avoid bumping into them. It should also be able to transport, pick up, and deliver material throughout the different work groups. It should be able to do all of this autonomously.

As for more specific requirements, the AGV should be designed so that it can be built using TechneLean material from the company Quimilock, since this type of material is readily available at TAP, and preferably it should be made the most use out of what already exists at the workshop. Also, the introduction of the AGV in the workshop should not interfere (or the interference should be minimized) with the current mode of operation in the workshop, which is to say, the AGV should be adapted to the workshop and the workers and not the other way around. In terms of battery life, the AGV should be able to work a full shift, but should also have an autonomous charging scheme, and should be able to take any opportunity to charge the battery.

While a budget was not defined for the design of the AGV, an effort should be made in keeping the design simple and affordable.

3.4 Previous Work

The introduction of an AGV on this particular workshop at TAP is a project that has already seen some study. Prior to this thesis, Enrique Serrano Martínez [5] already wrote a thesis where a preliminary design for the AGV's system was made.

This thesis will thus largely lean on the conclusions taken in the aforementioned study, but also build on it. Modifications will also be made whenever they seem necessary.

Martínez's thesis [5] focused on the study of the different types of AGV, navigation technology, types of guide path configuration, wheel configuration, types of battery and charging scheme, number of AGVs necessary, and concluded with a preliminary design of the AGV. Market studies were also performed in order to chose components and estimate costs. A summary of his conclusions will be presented throughout this section.

3.4.1 Guide Path Configuration and Navigation

The choice was made that the AGV will follow a closed path instead of an open one. This means that, instead of being able to navigate freely within the workshop through laser triangulation or natural navigation, the AGV will follow physical guidelines which define a specific path, from which the AGV can not stray from. The reason behind this choice was that, since the AGV is expected to always head towards the same locations, there is no need for the type of flexibility that an open path offers, which would also be more costly to implement. Besides, it's safer for the workers if the AGV is confined to a specific path instead of roaming free through the workshop, as it reduces the likelihood of collision. It also becomes less likely that the AGV will find obstacles, as workers should be instructed not to leave objects in the path.

The navigation system chosen was magnetic tape, since it's easy to install and modify while still being more reliable than some of the alternatives. This is because magnetic tape doesn't need to be embedded or painted on the floor, and can be easily removed and reapplied in case a change in path is desired. Also, because it depends on the magnetic properties of the tape, its detection isn't affected by dirt or dust, unlike a solution based on optical detection. The products chosen were thus the MGS1600GY sensor and the MTape25NR tape, both by company ROBOTEQ. The company also provides magnetic markers, which are strips of magnetic tape of opposite polarity to the guiding tape. These can be placed on either or both sides of the tape, and it is used to give information regarding the location of the AGV along the track or to give instructions.



Figure 3.6: Magnetic tape and sensor [17]

As for the path configuration, the decision was made that there would be a single unidirectional lane which would form a single loop that would go through all the areas, as can be seen in Figure 3.7.

This was the alternative that used the least amount of tape, the only disadvantage being that it's also

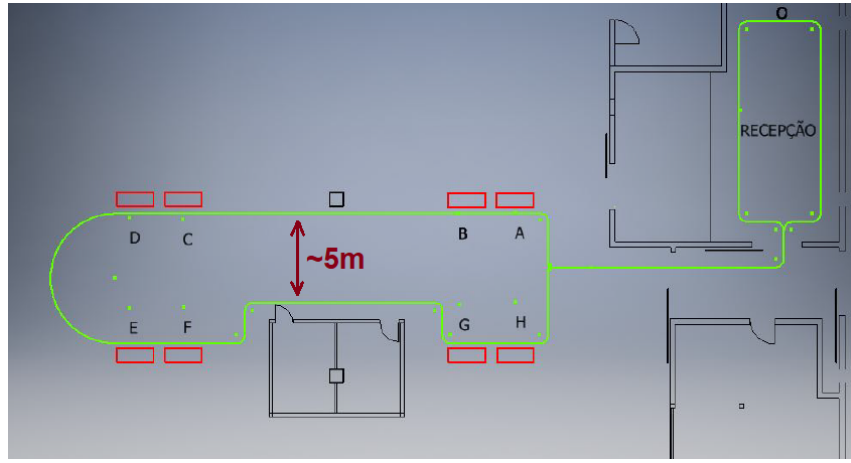


Figure 3.7: Single loop path with a single unidirectional lane [5]

the one that will force the AGV to always take the longest path. This may sound counterintuitive, but the explanation is that the alternative would be to create extra paths to allow the AGV to take shortcuts in case there were no trays to deliver to certain areas. This would possibly also complicate the project, because it's not always easy to predict what type of material is going to be available for delivery nor when, which would mean that the AGV would constantly need to receive new instructions on what path to take for each delivery. Nonetheless, this is the least consequential choice to make since, as it was stated before, magnetic tape is easy to apply and remove, so if in the future the company sees fit that a different path is needed, that can easily be done. So for now, it makes sense to make the simplest and cheapest choice.

3.4.2 Vehicle Type and Wheel Configuration

The type of AGV selected was the underride AGV, which is a type of vehicle that will place itself under the cargo which is meant to carry and lift or tow it from under it. Its advantages include it being compact, since it doesn't need to occupy an area much bigger than the cargo itself, its high manoeuvrability, and the quick loading and unloading. An example of an underride AGV can be seen in Figure 3.8.



Figure 3.8: Example of an underride AGV carrying a cart [18]



Figure 3.9: HYMO AXX4-8/6 P Lifting Table [19]

It was also decided upon using a lifting device, since it would allow the AGV to potentially be used to carry other types of material if the company saw necessary. The HYMO AXX4-8/6 P lifting table, which can be seen in Figure 3.9, was selected. The information regarding this product can be consulted in Table 3.1

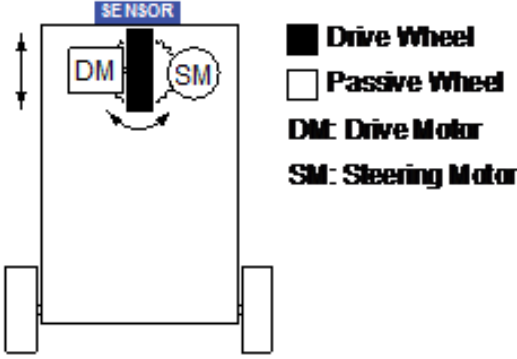


Figure 3.10: Tricycle configuration (adapted from [20])



Figure 3.11: C.F.R. Steerable drive wheel [21]

As for the wheels, a tricycle configuration was chosen, which consists of one wheel at the front connected to a drive motor and a steer motor and two supporting wheels at the back, as seen in Figure 3.10. This is the configuration that allows for the most precise steering and it's the most commonly used in AGVs of this type. Mecanum wheels were considered, but the idea was discarded due to their high cost. The motorized wheel chosen for this application was the one by the Italian company C.F.R., depicted in Figure 3.11. Table 3.2 lists some of the characteristics of the model MRT 10 DC002, which was the model suggested to Martínez by the company.

Table 3.1: AXX4-8/6 P Lifting Table information

Max. Load (kg)	400
Table size L x W (mm)	800 x 600
Height (mm)	200
Lift stroke (mm)	800
Lift time (s)	32
Control voltage (V)	24 DC
Supply voltage (V)	230 AC; 1-phase
Power (kW)	0.55
Total weight (kg)	120

Table 3.2: Steerable drive wheel information

Wheel diameter (mm)	196
Material	Polyurethane
Max. Load (kg)	550
Voltage (V)	24 DC
Motor Speed (rpm)	2500
Gear ratio	1:20
Power (W)	400
Total weight (kg)	42

3.4.3 Battery Type and Charging Scheme

For this type of vehicle, the use of rechargeable batteries was more convenient. Lead-acid batteries have been the most commonly used in this type of application, mostly because they are also the oldest type of rechargeable batteries, having been invented in 1859. However, it was ultimately decided that a lithium-ion battery would be used. While some relatively recent literature doesn't consider lithium-ion as an option for AGVs [1], others have verified that the use of this type of battery on this type of vehicle is ever growing [4]. This is because lithium-ion batteries offer a much higher energy density than other

rechargeable batteries, but at a much higher cost [6]. However, the price has been decreasing, and is expected to continue decreasing.

Lithium-ion batteries also have the added bonus of not having memory effect, so it should be possible for the AGV to have an opportunity charging scheme. Opportunity charging consists in taking advantage of idle time in between activities to charge the battery, even if not fully, instead of having to take necessary breaks to completely charge the battery.

The battery selected by Martínez [5] was the U1-24RT from the Company Valence.

Table 3.3: U1-24RT characteristics

Voltage	Capacity	Weight	Dimensions L x W x H	Max. Current	Charge Voltage	Energy
24 V	20 Ah	6.4 kg	197 x 131 x 183 mm	30 A	29.2 V	512 Wh

3.4.4 Fleet Size

Since the AGV is only expected to deliver a portion of the material that comes through the workshop (seeing as it will only be delivering to four of the areas), and since the current mode of operation in the workshop doesn't allow for a lot of material to be delivered in each route, then it isn't predictable that more than one AGV will be needed at this stage.

3.4.5 Safety Devices

Since the AGV will be operating in a workshop where a lot of people circulate and where there are a lot of potential obstacles, it's important to take safety measures so that no one is hurt and no material is damaged. The AGV should then be equipped with:

- An optical sensor – placed at the front of the AGV to scan for obstacles in the way. The sensor should allow for the distinction between a warning zone and a danger zone. When an obstacle enters the danger zone, the AGV should stop until the obstacle is moved out of the way. The product selected for this purpose was the S3000 standard safety laser scanner by the company Sick [5].

Table 3.4: S3000 standard safety laser scanner information

Protective field range (m)	4
Warning field range (m)	up to 49
Number of fields	4
Distance range (m)	49
Scanning angle (°)	190
Supply voltage (V)	24 DC
Weight (kg)	3.3

- A horn – to send out a warning when something enters the warning zone, and to send out repeated warnings when an obstacle in the danger zone is stopping the AGV from moving.

- Lights – so that there is a visual warning of the presence of the AGV.
- An emergency stop button – to shut down the AGV in case of an emergency.

3.4.6 Preliminary Design

Having chosen the AGV's components and knowing their dimensions and weight (which can be conferred in Table 3.5), Martínez [5] then proposed a design for the AGV, starting by sketching out the main components' relative placement, which can be seen in Figures 3.12a and 3.12b, and then coming up with a concept for the chassis, seen in Figures 3.12c and 3.12d. Finally, a concept for the finalized look of the AGV can be seen in Figures 3.12e and 3.12f. The material used to design the chassis was a square steel tube with black zinc coating, with a 45x45mm section and a 2mm thickness, which is named HL-220 on the TechnoLean catalogue.

Table 3.5: Components information

Device	Brand and Model	Dimensions L x W x H (mm)	Weight (kg)
Lifting table	HYMO AXX4 - 8/6	800x600x200	120
Battery	Valence U1-24RT	131x197x183)	6.5
Steerable drive wheel	C.F.R. MRT 10 DC002	350x361x249	42
Safety sensor	Sick S3000 standard	160x155x185	3.3
Magnetic sensor	Roboteq MGS1600GY	30x165x25	0.25

Table 3.6 displays the final dimensions of the AGV, as well as the weight. The final weight, however, does not take into consideration the weight of the chassis.

Table 3.6: Vehicle total dimensions

Length (mm)	Width (mm)	Height (mm)	Weight (kg)
1875	600	294	172.05

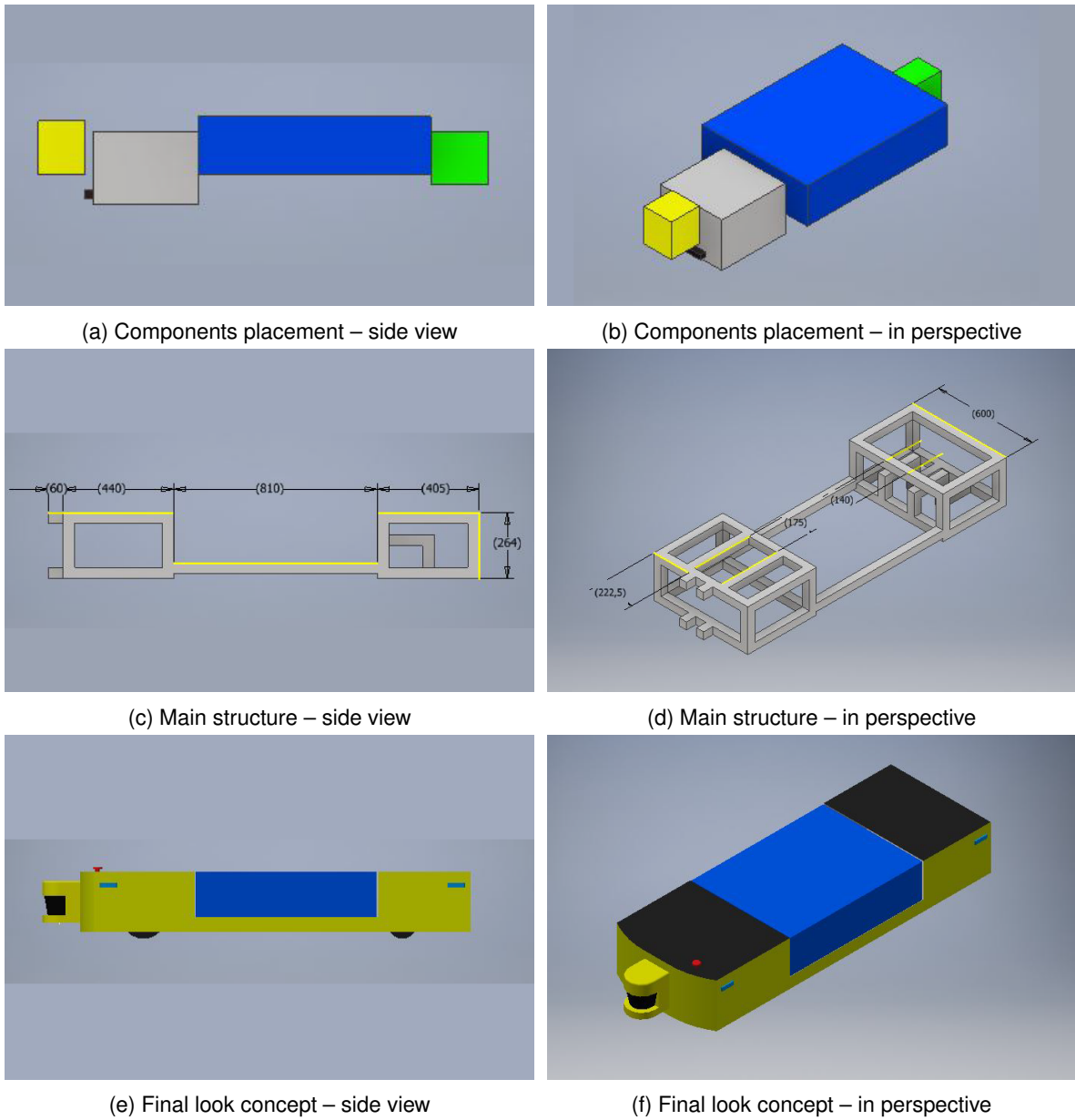


Figure 3.12: Preliminary design of the AGV (adapted from [5])

Chapter 4

Material Distribution System

4.1 Analysis of the Preliminary Design and Concept Adaptations

The main focus of Martínez' thesis [5] was to take conclusions on what type of AGV and technology would be more fitting for the application in cause, which is very important and relevant work. This now leaves the task of analysing the loads involved to guarantee that the AGV is not only structurally sound, but also that the electronic components, such as the motor and batteries, are appropriate for the task.

One of the main downsides of Martínez' [5] preliminary design was the fact the the vehicle was very long. The carts that the AGV is supposed to carry are 920mm long, making the AGV almost a full meter longer than its cargo, with a length of 1875mm. This could be a problem mainly due to the fact that the RE area is not very spacious, and the AGV should be able to circulate in this area. However, the preliminary design is completely restrained by the dimensions of its components, namely the lifting table, which is the biggest component in the AGV.

As it was explained in section 3.4.2, the decision to use a lifting device, as opposed to a towing device, was based on the possibility of the AGV being used to carry other material in the future. It makes the AGV more versatile, but, in the scope of this project specifically, the lifting table isn't a necessity. Since the carts have wheels, there should be no reason why the AGV couldn't rely on a towing device. For these reasons, the decision was made to change the type of AGV from a lifting underride to a towing underride. This decision also has the added bonus of making the AGV much lighter, since the lifting table was not only the biggest component, but the heaviest as well, weighing 120kg. The reason this is a good thing is related with the dimensioning of the motor.

As stated in section 2.1.4, the tractive effort, which is the force that propels the vehicle forward, is the result of a torque being applied to the wheels by a motor. From equation (2.11) it's clear that the torque will increase when the tractive effort increases, and, from equation (2.8), it's possible to conclude that the tractive effort will depend on the mass of the vehicle. As seen before in equation (2.12), the torque a motor outputs is directly related to the power it draws. As such, a lighter vehicle will allow for a less powerful motor, which in turn will need less powerful batteries, which will likely translate in a reduction in the cost of the AGV.

As an alternative to the towing vehicle, another solution was considered, which was to merge the AGV and the cart, i.e., to eliminate the existing carts and instead create an AGV that already incorporates shelves to carry the trays. This would be a very interesting solution, as it would make it easier to equip the shelves with sensors which could communicate directly with the AGV's controller and allow it to make more customized decisions. However, one big downside to this solution is that there would have to be as many AGVs as carts, since there are usually a few carts that are being prepared simultaneously. This would mean that the investment the company would have to make to implement the AGVs would be much higher. It was also considered the possibility of still making the cart and AGV separate from each other, but have them still be able to connect somehow, whether it be through Wi-Fi or through some kind of contact connection.

However, these last two solutions would shift the main focus of this project to programming and control based solutions, which was not the point of this thesis. For this reason, it was ultimately decided that these solutions would not be pursued in this thesis, but they remain worth mentioning as a suggestion for future developments.

4.2 Cart Adaptations

4.2.1 Current Carts and Cargo

A schematic of the carts being currently used can be seen in Figure 4.1, and a picture has been shown previously in Figure 3.4.

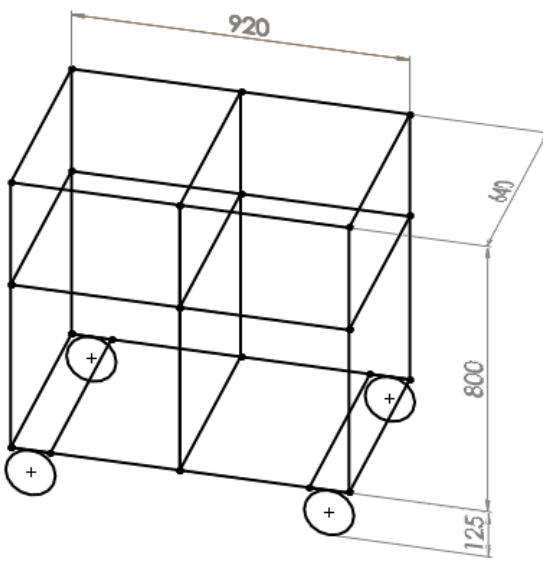


Figure 4.1: Cart dimensions in mm



Figure 4.2: Back view of the cart

The carts were built using only TechnoLean material, and consist of a combination of tubes connected by joints, all made of steel. They are supported by four swivel castors connected to corner plates.

As can be seen in Figures 3.4 and 4.2, the carts have two levels of shelves, with two shelves each. Each shelf can fit one 600x400 mm tray or combinations of smaller trays, up to four 300x200 mm trays, meaning each cart has enough room to carry as little as four 600x400 mm trays or as many as sixteen 300x200 mm trays.

The shelves of the carts are composed of inclined roller tracks that are limited laterally by descend guides, as can be seen in Figure 4.2. This inclination is achieved through the use of connectors with different heights, as seen in Figure 4.3. These connectors make it so the trays aren't able to slide off the shelf. Considering the dimensions of the cart and of the connectors, the inclination of the shelves is of about 3°.

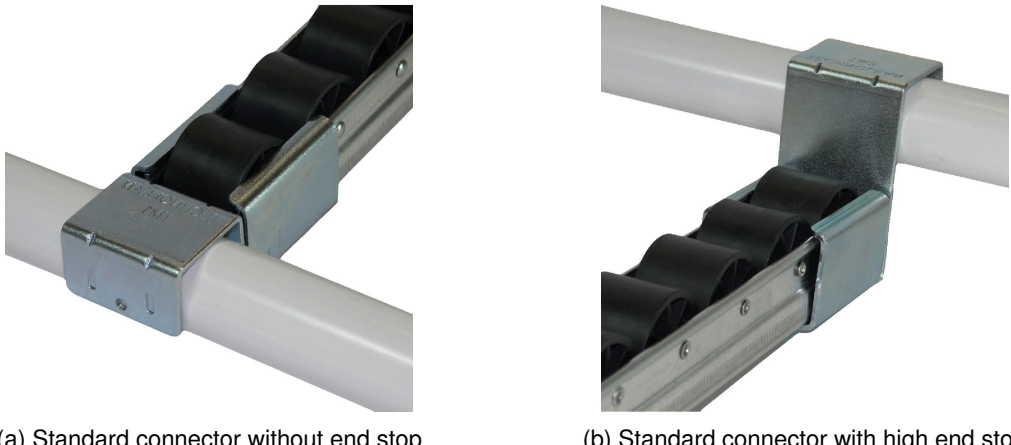


Figure 4.3: Connectors [22]

There were no means at the workshop to allow for the weighing of a cart, so this weight had to be estimated. The tubes have an outer diameter of 28.6 mm and have a thickness of 1 mm or 2 mm. Knowing how many tubes were used, and the thickness and length of each one, the calculated volume of tube used was of $V = 2.4 \times 10^6 \text{ mm}^3$. Since the structure is entirely made of steel, a typical value of $\rho = 7.9 \text{ g/m}^3$ was considered for the density.

$$\rho = \frac{m}{V} \quad (4.1)$$

Converting these values to the relevant units and applying equation (4.1) results a mass, m , of approximately 19 kg. This doesn't account for any other elements beside the tubes, so a conservative estimate was made that the total weight of the cart would be of 38 kg, meaning the distribution of mass of the cart would be 50% tubes and 50% everything else.

As for the cargo, according to the workers, the heaviest component they carry in the carts weighs about 30 kg, and that, at most, they would carry two at a time in a single route. They also assured that, besides those two components, the rest of the cargo would not surpass 10 kg. So it was defined that the maximum weight carried by the car would be of 70 kg. This would amount to a total weight of 108 kg between cart and cargo.

As was also mentioned before, in the workshop there are expedition and reception stations in each of the groups, seen in Figure 3.5. These stations have a similar structure to the ones in the cart, in

the sense that they also have inclined shelves composed of roller tracks. What differentiates them from each other is that the shelves from the reception station are inclined away from the corridor, so that the trays slide in the direction of the work area, and the expedition station's shelves are inclined towards the corridor. Their placement in the workshop and relatively to the path of the AGV can be seen in Figure 3.7, where A, C, E, and G are reception stations, and B, D, F, and H expedition stations. The path of the AGV will thus follow along the stations from A to H, and it can be seen the stations will be to the right of the AGV as it passes by them.

The inclining of the shelves is a simple example of a tool that has been used in Kaizen applications called "Karakuri". Karakuri is the Japanese word for "mechanism". Between the 17th and 19th century, it was used mainly in puppets for entertainment purposes. Nowadays, it consists on the use of automated mechanisms that rely solely on physical principles, and don't require any type of sensors or electric power sources [23–27]. In this case, the movement of the trays relies solely on the force of gravity.

4.2.2 Distribution System

The goal of this project was to project a transporting system capable of autonomously distributing material. Seeing as the cart is the component that carries this material, it was necessary to make modifications to the cart so as to equip it for this task. To avoid having to add an electric power source to the cart, the challenge was taken on to try and make this system completely mechanic, thus staying true to the Karakuri method.

For starters, one obvious change that needed to be made to the cart was the possibility for the trays to slide off of the shelves. For this, a simple change of the connectors that secure the rolling tracks was needed, where the connector from Figure 4.3b would be replaced by a connector from Figure 4.3a, and the connector from Figure 4.3a would be replaced by a connector from Figure 4.4. It was determined that this solution would slightly alter the inclination of the shelf to about 3.1° , which would not significantly affect the sliding speed of the tray.



Figure 4.4: Intermediate support type connector [22]

The cart should thus approach the reception shelf, moving parallel to it, and stop in front of it, so that the shelves of the cart align with the shelves of the reception station. The trays should then slide from the side of the cart to the reception station's shelves, as can be seen schematically represented in Figure 4.5.

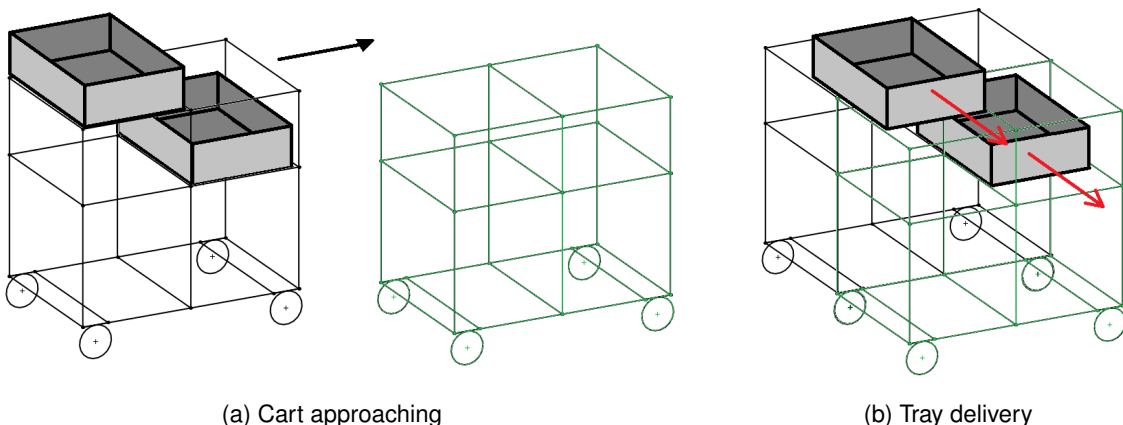


Figure 4.5: Tray delivery. Cart is represented in black and reception shelf is represented in green

Now, a solution to control the sliding of the trays was necessary. After some research, one by the company item was found, which can be seen in Figures 4.6 and 4.7.

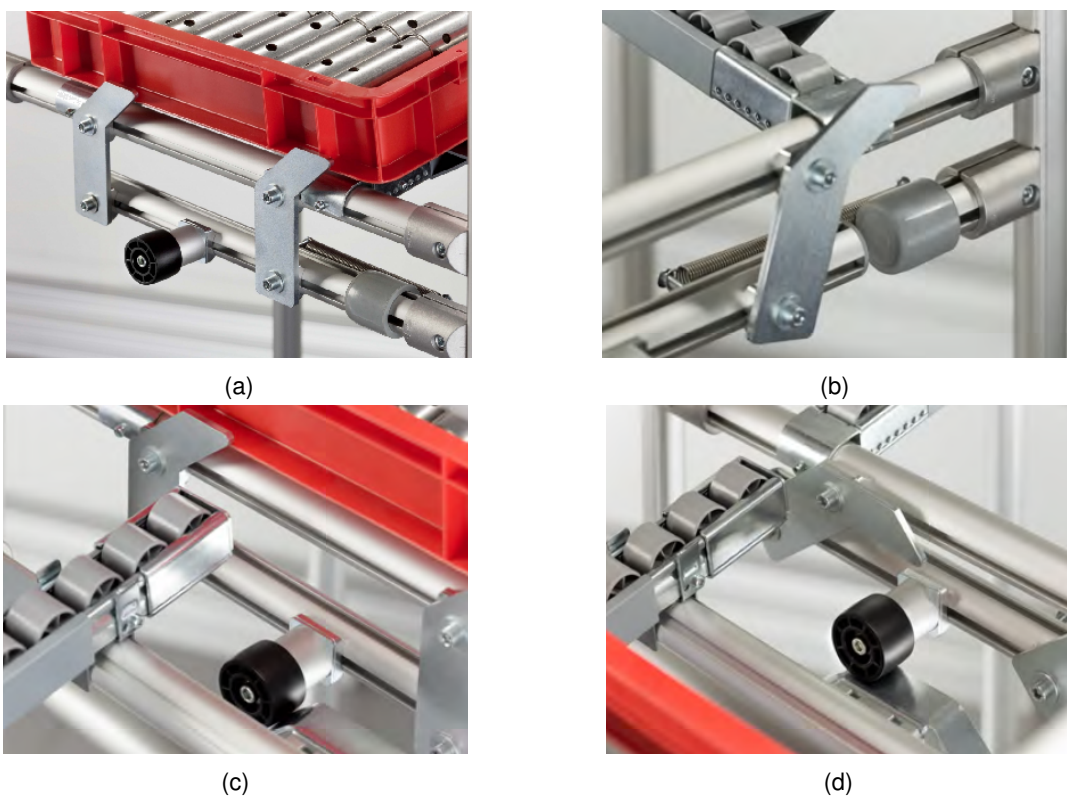


Figure 4.6: Pictures and schematics of the mechanism [28]

Simply explained, this mechanism consists of a number of stoppers that prevent the tray from sliding off the inclined shelf. The stoppers can rotate around an axis and are connected to a bar that has a protruding roller. When the cart approaches the receiving shelf, the roller will come into contact with a ramp, forcing the stoppers to rotate and allowing the tray to slide freely. The stoppers are then brought back to their original position by a spring.

The company item is a direct competitor of Quimilock, and both companies sell many similar products

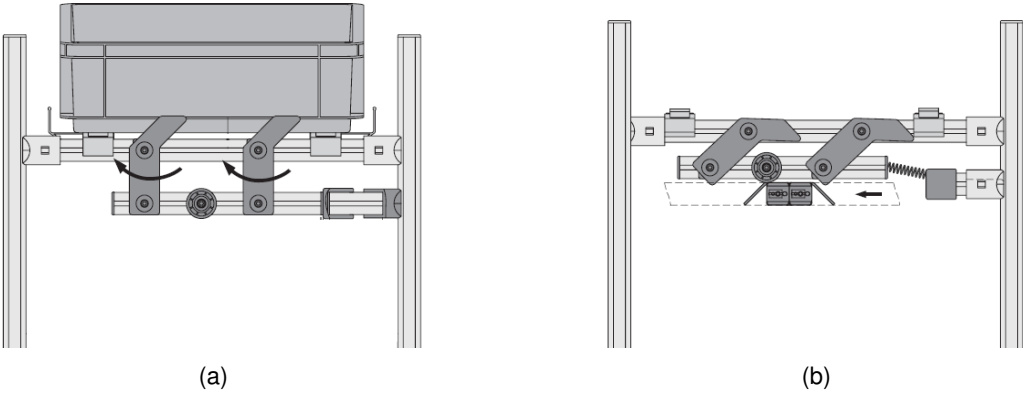


Figure 4.7: Pictures and schematics of the mechanism [28]

with the same purposes. For this reason, it seemed reasonable to contact Quimilock to ask if it had any parts to create an assembly that resembled this one. Unfortunately, the company didn't have any specific parts to assemble a mechanism like this one, but they did provide an example of how their material could be used to achieve a similar result, seen in Figure 4.8.

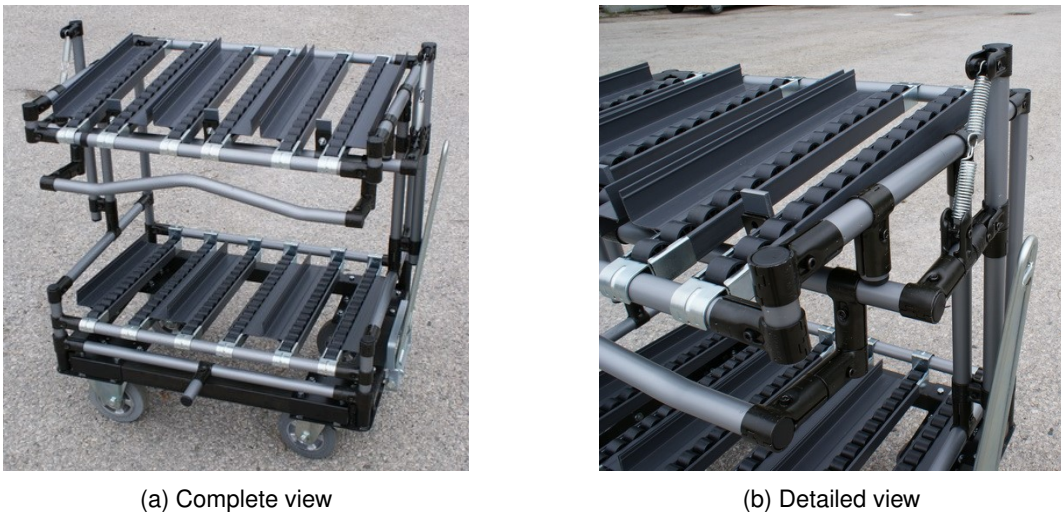


Figure 4.8: Solution provided by Quimilock

Besides the solution provided by the company, an attempt was still made to recreate the mechanism from the company item using TechnoLean material. The result, which will henceforth be referred to as lock, can be seen in Figure 4.9.

This mechanism uses four rotating connectors, which can be seen in Figure 4.10, and two parts forming a 'T' joint. As for the roller, one possible option would be to use a wheel that is used for the roller tracks, seen in Figure 4.11.

Because this lock is completely mechanic, it was necessary to ensure that each tray would only be released at the right time, i.e., that each of the cart's shelves would only be triggered to open by the correct receiving shelf, and no other. A simple way of achieving this would be to place the roller of each lock, as well as the activating ramps on each of the groups' reception shelves, at a different height, so that each roller would only come into contact with a ramp at that specific height and miss all the others.

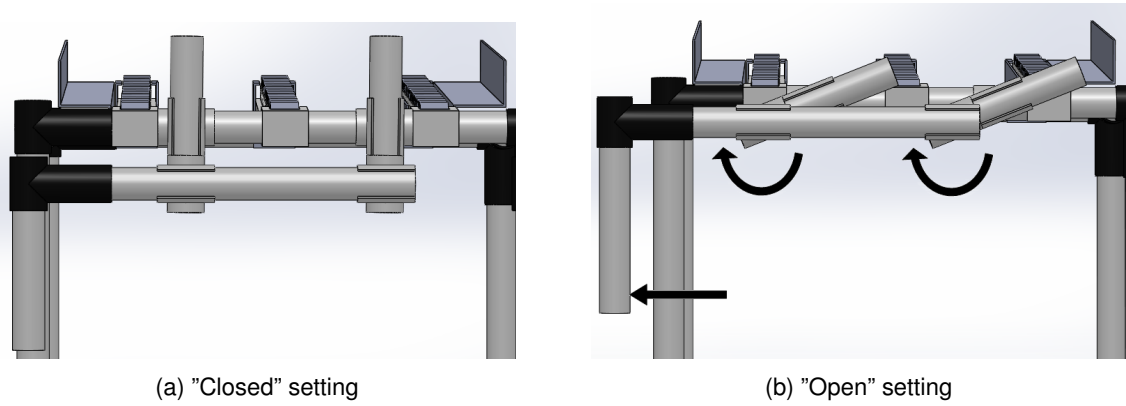


Figure 4.9: Locking mechanism



Figure 4.10: Rotating connector (image from [22])

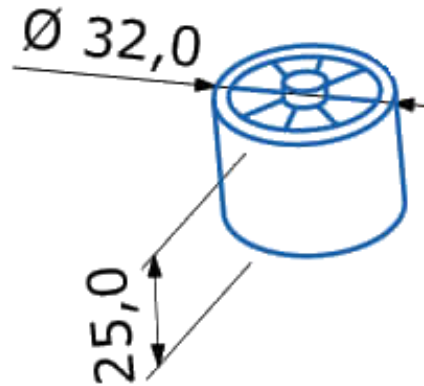


Figure 4.11: Roller wheel schematics (adapted from [29])

This can be seen represented in Figure 4.12. For the sake of clarity, the schematics from item were made use of for the picturing of this solution.

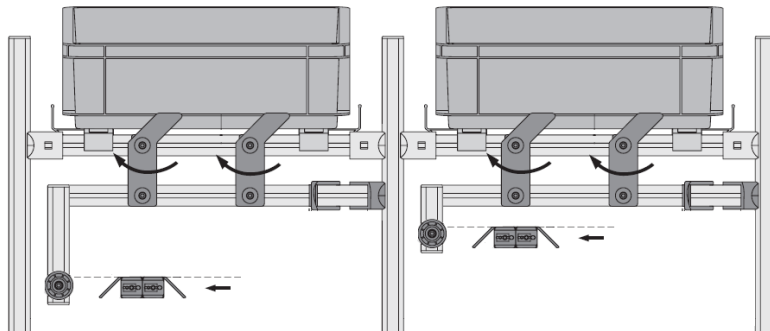


Figure 4.12: Rollers at different heights (adapted from [28])

This would mean that each of the cart's shelves would have to be reserved to a different group, which would be appropriate if the amount of material to be delivered to each of the groups was mostly even on most of the routes. However, according to the workers who perform these routes, this is not usually the case, meaning that more often than not, the AGV would have to perform routes with a mostly empty

cart, and would have to do extra routes to make sure to deliver all of the material.

Another possible solution would then be to make the roller adjustable in height, for example, through drilling holes at different heights on the vertical arm of the lock, where the roller would then attach, as can be seen in Figure 4.13. This way, each position of the roller would correspond to a different area, and every shelf could carry any colour of tray.

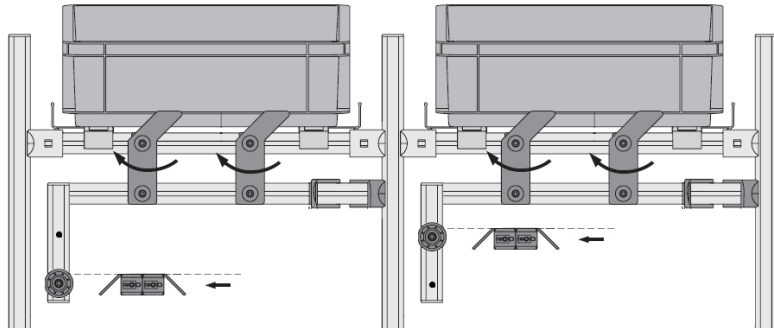


Figure 4.13: Adjustable rollers (adapted from [28])

Since this solution would allow for the possibility of all shelves carrying trays to one single group, then the receiving shelves should be made compatible with the cart, having the same two levels with two shelves each.

Potential Conflicts and Resolution Suggestions

The last solution suggested implies that the vertical arm of the lock should have four different height settings for the roller, one for each group. However, if these four levels are the same for all the locks, then, for two shelves at the same level, if the rollers were placed at the same height, that would lead to those shelves being activated more than once. This is only a problem if a lock is activated by a shelf prior to its destination shelf, which would lead to a tray being delivered to the wrong place. If a lock is activated after its tray has been delivered then there are no consequences.

One possible solution would be to add a vertical offset to misalign the levels of the rollers for same level locks, as shown in Figure 4.14. For this, it should be ensured that there are no interferences between the rollers and the activating ramps of different levels, or, at least, the interference should be as small as not to trigger the complete opening of the lock.

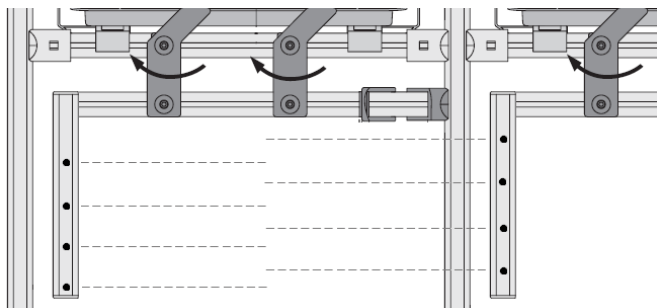


Figure 4.14: Vertical misalignment (adapted from [28])

This could also be achieved with a horizontal offset, in which the roller levels would still be aligned vertically, but on the locks from the cart's rear shelves, the rollers' notches would be more protruding than the aft shelves, and their corresponding activating ramps should be recessed, so that they only activate the locks of the rear shelves. A schematic can be seen in Figure 4.15.

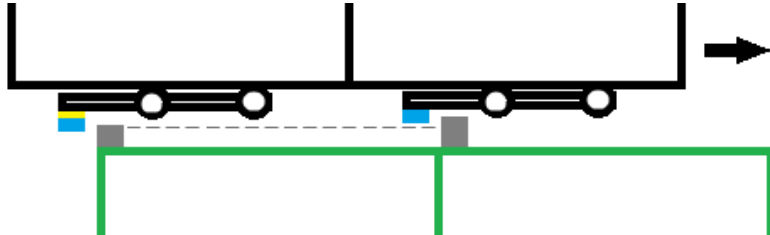


Figure 4.15: Schematic view from above. The reception shelves are represented in green, the ramps in grey, the rollers in blue, and the offset in yellow. The arrow represents the direction of motion of the cart

Figure 4.16 displays a schematic example of how the rollers and ramps could be placed, where the vertical rectangles on the left represent the two locks and the four different levels for the rollers, and the numbers represent each of the groups, and on the right are represented the groups' reception stations, where the diagonal lines represent the activating ramps.

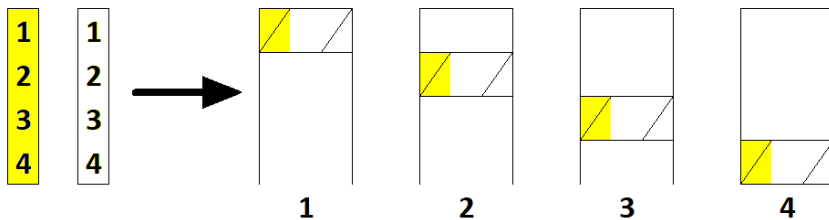


Figure 4.16: Horizontal misalignment. The yellow shaded areas represent the rollers and ramps that have an offset, and the arrow represents the direction of motion of the cart

Considering an example where two trays are being carried to different groups, no interference will happen, because the rollers will be placed at different levels. If two trays are being carried to the same group, then as the cart approaches the reception station, the front locks' roller will miss the first ramp (shaded in yellow), which is recessed, as the cart aligns with the station, and will only be activated by the second ramp. When the trays are delivered and the cart moves away from the station, the rear lock will be activated by the second ramp. However, this won't constitute a problem, as the cart's shelf will be empty.

4.2.3 Expedition System

Until now, the focus has been on figuring out the delivery of material to the four groups. But, besides this, the AGV is also expected to aid in retrieving trays containing repaired parts and take them back to the RE area.

As was explained before, both the reception and expedition stations will be to the right of the AGV, and it was also mentioned that what differentiates them is the direction to which their shelves are inclined. The cart, however, will have all the shelves inclined the same way, so for it to be able to receive trays

from the expedition stations, the cart would have to be turned around. Because this can't be done during a route, the reached solution requires the distribution of trays and the collection of trays to be done in separate routes.

In the routes where the AGV retrieves the repaired parts, the cart should thus be attached to the AGV in a backwards position, with the shelves descending to the left. The mechanism that allows the sliding of the trays from the stations' shelves to the cart would be the same as described before, using a combination of locks activated by ramps, but, in this case, the locks would be attached to the stations' shelves whereas the activating ramps would be on the cart.

In terms of real life functionality, since there is no way of knowing *a priori* how many trays there are in each group ready to be collected, then the best way to avoid any conflicts that may arrive from not knowing what shelves are going to become full in each station is to reserve each shelf to a single group. This would mean that in each expedition station, only one shelf would be activated by the cart, rendering the other shelves basically useless, from the perspective of the AGV.

One suggestion to counteract this problem would be to redesign the expedition shelves so that this single shelf would be automatically supplied with another tray whenever it was emptied by the AGV. Figure 4.17 shows the schematics for an example mechanism.

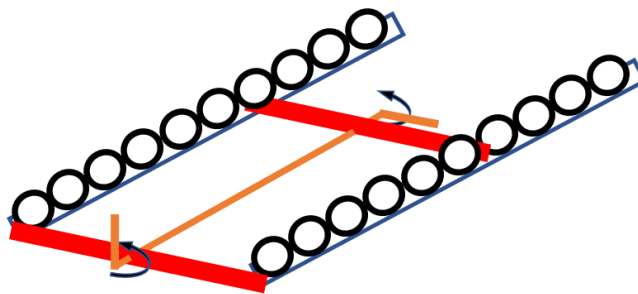


Figure 4.17: Example of mechanism for expedition shelves

Unfortunately, due to lack of time, it was not possible to further develop and concretize this solution, but it remained worth to mention, as it could be relevant for future developments.

4.2.4 Coupling

It was determined earlier, in Section 4.1, that the AGV would transport the carts by means of a towing device. A similar project [30] accomplished this by means of a towing pin, which was activated with the help of a linear actuator.

Since the carts are supported by swivel castors, to avoid the cart and the AGV to rotate relative to each other during curves, potentially causing collisions between the AGV's and the cart's structures, it was decided that the use of two pins would be better than just one.

The coupling between the AGV and the cart should be done automatically. The cart that is meant to be transported should be placed by a worker in a designated area, that should be clearly outlined, and

where there should be markers to instruct the AGV to activate its pins.

Figures 4.18a and 4.18b portray the suggested design of the coupling structure.

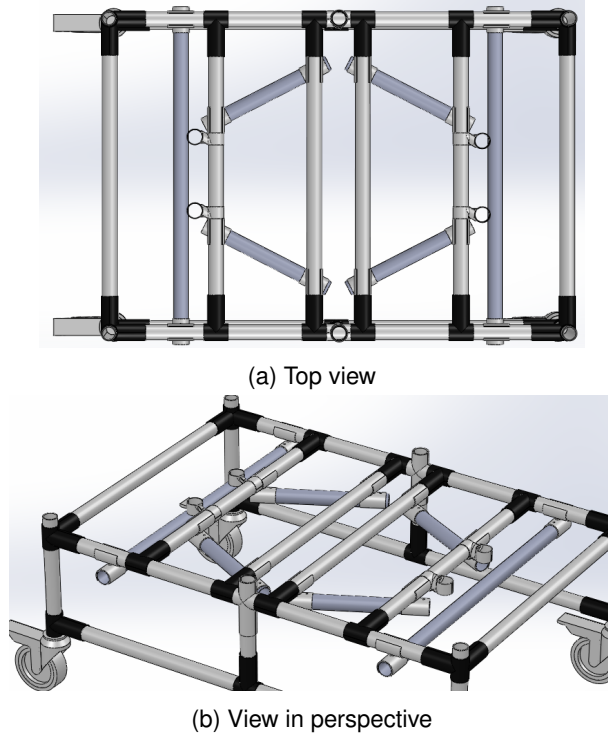


Figure 4.18: Coupling structure (sectioned view)

As can be seen, the structure is symmetrical, so that the AGV can attach to the cart in both directions, so as to accommodate the separation of the distribution and collection routes. The diagonal pieces that appear in the design should serve as guides for the towing pins, in case the cart is placed slightly misaligned. At the end of those guides, there are two 90° crossover tube joints, where the pins will hook on to. As can also be seen, the guides and the hooks are at different heights, so the towing ping should be capable to adjust in height. This means that instead of a linear actuator, it will likely be necessary a linear servo to control the height of the pin.

As well as the addition of this structure, in order to allow the AGV to go under the cart, the current castors should be replaced by castors that don't require corner plates, and instead connect to the tubes with a plug-in pin, like the one seen in Figure 4.19.



Figure 4.19: Castor with tube plug-in pin [31]

4.2.5 Final Cart Design

The general look of the final design of the cart can be seen in the following images.



Figure 4.20: 3D drawings of the cart (dimensions in mm)

4.3 Designing the AGV

4.3.1 First Considerations

The material chosen for the preliminary design of the AGV was mentioned previously in Section 3.4.6 as being steel tube of square section. This material is under the Heavy Load category on the TechnoLean catalogue, and is not a type of material that is readily available at TAP. While it made sense to use this material for a lifting type AGV, since the current concept will be subjected to lighter loads, the design will be made assuming the use of the same type of material used to build the carts.

4.3.2 Equations of Motion

As was explained in Section 2.1, to model an electric vehicle one must know how its motion relates to the forces that it's going to be subjected to. In that section, equation (2.8) was defined as a general equation that describes just that. It is now imperative to apply and further expand that equation so as to fit the specific case of this project.

Figures 4.21a and 4.21b display the free body diagrams of the AGV and the cart, respectively.

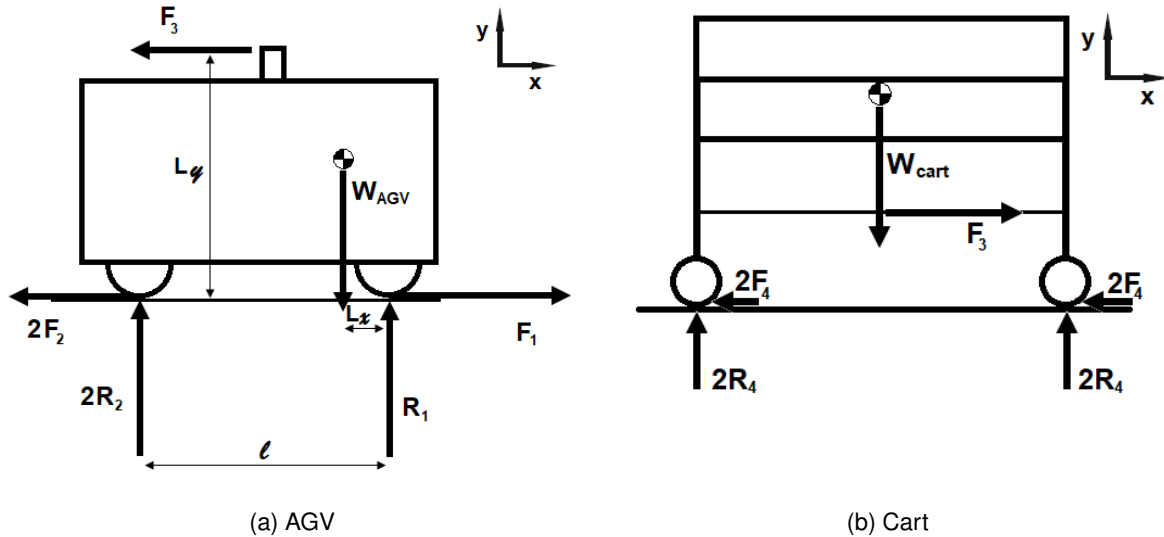


Figure 4.21: Free body diagrams

where F_1 = tractive effort

F_2, F_4 = rolling resistance of each individual pulled wheel

F_3 = force pulling the cart

R_1, R_2, R_4 = normal reaction of the wheels

$W_{AGV} = m_{AGV}g$ = total weight of the AGV

$W_{cart} = m_{cart}g$ = total weight of the cart (including load)

L_x = horizontal distance between front wheel and center of gravity of the AGV

L_y = vertical distance between F_3 and ground

l = horizontal distance between front wheel and back wheels of the AGV

Right away, it's possible to see a parallel between Figure 4.21a and Figure 2.1, except that both the aerodynamic drag and the slope are missing. This is because the ground is plane all throughout the workshop, so the AGV is not expected to encounter any slopes. Besides this, the AGV will not move at great speed, so the aerodynamic drag will be very small in comparison to the rest of the forces. Thus, these two components were disregarded to simplify the calculations.

Applying equation (2.8) results:

$$F_1 = m_{AGV}a + 2F_2 + F_3 \quad (4.2)$$

where m_{AGV} is the mass of the AGV, and a is its acceleration.

Applying the equations of motion and calculating the sum of moments on the contact point between the front wheel and the ground results:

$$\sum F_y = 0 = R_1 + 2R_2 - W_{AGV} \Leftrightarrow R_1 = W_{AGV} - 2R_2 \quad (4.3)$$

$$\sum M_1 = 0 = 2R_2l - W_{AGV}L_x - F_3L_y \Leftrightarrow R_2 = \frac{F_3L_y + W_{AGV}L_x}{2l} \quad (4.4)$$

And using the formula (2.3) for the rolling resistance to the back wheels of the AGV:

$$F_2 = I_2 \frac{a}{r_2^2} + \mu_{rr,2} R_2 \quad (4.5)$$

Similarly, for Figure 4.21b result the following equations:

$$\sum F_x = m_{cart}a = F_3 - 4F_4 \Leftrightarrow F_3 = m_{cart}a + 4F_4 \quad (4.6)$$

$$\sum F_y = 0 = 4R_4 + -W_{cart} \Leftrightarrow R_4 = \frac{W_{cart}}{4} \quad (4.7)$$

$$F_4 = I_4 \frac{a}{r_4^2} + \mu_{rr,4} R_4 \quad (4.8)$$

The equilibrium of moments for the cart was not calculated because it is not of relevance to calculate the normal force for each one of the cart's wheels. For the purpose of the calculations, it is going to be assumed they are all of equal value, as Equation 4.7 implies. The reason for this is that, even though the load on the cart may not be evenly distributed, because the wheels are all the same model and have the same properties, the distribution of the load will not affect the resultant of the friction force.

Equations (4.2) through (4.8) result in the system of equations (4.9), which defines the kinetics of the AGV.

$$\left\{ \begin{array}{l} R_4 = \frac{W_{cart}}{4} \\ F_4 = I_4 \frac{a}{r_4^2} + \mu_{rr,4} R_4 \\ F_3 = m_{cart}a + 4F_4 \\ R_2 = \frac{F_3L_y + W_{AGV}L_x}{2l} \\ R_1 = W_{AGV} - 2R_2 \\ F_2 = I_2 \frac{a}{r_2^2} + \mu_{rr,2} R_2 \\ F_1 = m_{AGV}a + 2F_2 + F_3 \end{array} \right. \quad (4.9)$$

4.3.3 First Design Iteration

In order to solve (4.9), some values need to be defined or assumed.

Previously in Section 4.2.1, it was defined that the maximum weight of the cart plus the cargo would be of around 108 kg.

The cart's wheels and the AGV's back wheels are both swivel castors with rubber wheels of similar mass and radius, meaning their moments of inertia will be the same. The radius of the wheels is 50 mm and its mass was assumed to be approximately 0.5 kg. To simplify, it'll be assumed their moment of inertia is approximately the one of a solid cylinder [11].

$$I_2 = I_4 = I = \frac{1}{2}m_{wheel}r_{wheel}^2 = \frac{1}{2} \times 0.5 \times (0.05)^2 = 0.000625 \text{ kg} \cdot \text{m}^2 \quad (4.10)$$

As for the weight of the AGV, Table 3.5 provides the weight of a few key components to be used on the AGV, namely the battery, the sensors, and the drive wheel, which summed up weigh approximately 52 kg. To account for the structure of the AGV, a first estimate of 75 kg was considered for its total weight.

In terms of acceleration, the AGV's maximum speed should be about the same as the average walking speed of an adult human. According to data collected by Levine and Norenzayan [32], that speed varied from 1.09 m/s in the slowest country to 1.64 m/s in the fastest. So the chosen speed for the AGV was of 1.4 m/s. Since the AGV isn't going to achieve high speeds, there's no need for a very high acceleration, so an acceleration of 1 m/s² was assumed.

Dimensions L_x , L_y and l were defined as 0.2 m, 0.3 m, and 0.9 m, respectively. While L_x was defined in a more or less arbitrary way, L_y was based on the expected height of the AGV, which can be seen on Table 3.6, and l is based on the length of the cart, seen in Figure 4.1.

For the values of $\mu_{rr,2}$ and $\mu_{rr,4}$, Table 4.2 shows some empirical values for different types of tires in different conditions. However, it's not clear what value should be used that would most approximate the conditions of this project. The values were thus calculated using equation (4.11), which was derived by Evans [33] for solid rubber tyres, assuming a rigid ground.

$$F_{rr} = \frac{h}{4.4} \left(\frac{P^4 t}{E s r^2} \right)^{\frac{1}{3}} \quad (4.11)$$

where F_{rr} = rolling resistance

h = fraction of energy dissipated

P = total vertical load on the wheel

t = thickness of the tyre

E = modulus of elasticity of the tyre

s = width of the wheel

r = radius of the wheel

Taking equation (4.11) and comparing with (2.3), assuming a constant velocity, and considering Figures 4.21a and 4.21b, results:

$$\mu_{rr,2} = \frac{h}{4.4} \left(\frac{R_2 t}{E s r^2} \right)^{\frac{1}{3}} \quad (4.12)$$

Table 4.1: Empirical values for rolling resistance coefficient [34]

Conditions	Rolling resistance coefficient
railroad steel wheels on steel rails	0.001 - 0.002
bicycle tire on wooden track	0.001
low resistance tubeless tires	0.002 - 0.005
bicycle tire on concrete	0.002
bicycle tire on asphalt road	0.004
dirty tram rails	0.005
truck tire on asphalt	0.006 - 0.01
bicycle tire on rough paved road	0.008
ordinary car tires on concrete, new asphalt, cobbles small new	0.01 - 0.015
car tires on tar or asphalt	0.02
car tires on gravel - rolled new	0.02
car tires on cobbles - large worn	0.03
car tire on solid sand, gravel loose worn, soil medium hard	0.04 - 0.08
car tire on loose sand	0.2 - 0.4

$$\mu_{rr,4} = \frac{h}{4.4} \left(\frac{R_4 t}{E s r^2} \right)^{\frac{1}{3}} \quad (4.13)$$

From taking measurements of the wheels, it is known that $t = 7.5$ mm, $s = 32$ mm, and $r = 50$ mm. The tyre is made of rubber. According to Cambridge University's "Materials Data Book" [35], the types of rubber mostly used in tyres are Butyl Rubber, Isoprene, and Natural Rubber, which have Young's moduli ranges of 0.001 - 0.002 GPa, 0.0014 - 0.004 GPa, and 0.0015 - 0.0025 GPa, respectively. To err on the side of caution, the lowest modulus of elasticity, 0.001 GPa, was used to calculate the rolling friction coefficients, as this will result in a greater rolling resistance. The h used was of 0.5.

With this, it is now possible to solve system (4.9) for all its variables. The results can be seen in Table 4.2.

Table 4.2: First iteration results

R_4 (N)	$\mu_{rr,4}$	F_4 (N)	F_3 (N)	R_2 (N)	R_1 (N)	$\mu_{rr,2}$	F_2 (N)	F_1 (N)
264.87	0.033	8.99	143.96	105.74	524.27	0.024	2.79	224.54

Calculating Torque and choosing the Motor

Having been calculated the tractive effort, it is now possible to calculate the corresponding necessary torque. The relationship between these two has been previously defined by equation (2.11).

The company C.F.R. srl was then contacted to ask for a new motor that would be more appropriate for this project, and the model MRT05.D0101 was suggested. The complete technical specifications of the motor can be seen in appendix A. Table 4.3 shows a summary of the most relevant specifications.

From Table 4.3 it is known that the wheel has a diameter of 198 mm, but no information is given about how much it weighs by itself, so an estimate was made of 5 kg. Assuming once again the moment of inertia of the wheel to be approximately the one of a solid cylinder, and applying equation (2.11) results:

Table 4.3: New steerable drive wheel information

Power (W)	400
Battery voltage (Vdc)	24
Speed (rpm)	2800
Current (A)	23
Max. wheel torque (Nm)	180
Nominal wheel torque (Nm)	29.5
Max. load (kg)	550
Wheel diameter (mm)	198
Material	Polyurethane
Total weight (kg)	42

$$T = F_1 r + I \frac{a}{r} = 224.54 \times (0.198/2) + \left[\frac{1}{2} \times 5 \times (0.198/2)^2 \right] \times \frac{1}{0.198/2} = 22.48 \text{ N} \cdot \text{m} \quad (4.14)$$

Seeing that in normal conditions the motor can continuously output a torque of 29.5 Nm, this gives a safety factor of 1.3.

Choosing the Batteries

It has been established that, while the AGV should have the ability to charge during its idle time, it should also be able to work a full shift without much interruption.

$$\text{run time}[h] = \frac{\text{battery capacity}[Ah]}{\text{circuit draw}[A]} \quad (4.15)$$

The run time of a battery can be calculated through equation (4.15), and Table 3.3 indicates the battery chosen by Martínez [5] has a capacity of 20Ah. While the final circuit that makes up the AGV is not yet been defined, it should be safe to assume that most of the circuit draw will be done by the motor, which, as seen in Table 4.3, is of 23 A in nominal conditions. Considering those two values, that results in a run time of about 52 minutes. This may be sufficient for a prototype, but for the finished product it's likely not enough. So instead, for the sake of the design and calculations, PowerBrick batteries by company PowerTech were considered. The batteries' specifications can be consulted in Table 4.4

Table 4.4: Lithium Ion battery 12V 70Ah – LiFePO4 – PowerBrick specifications

Voltage	Capacity	Weight	Dimensions L x W x H	Discharge Current	Max. Charge Current	Energy
12 V	70 Ah	9.8 kg	228 x 138 x 210 mm	65 A	35 A	896 Wh

Connecting the batteries in series gives a total battery capacity of 140 Ah, elevating the run time to approximately 6 hours. Previously, in Section 3.2, it was mentioned that the current routes take up 10 hours per day in total, but that the AGV is not expected to take charge of all of them. In reality, there are no current routes established that focus on the four groups alone, meaning that the routes will likely need to be adapted to the AGV, making it unclear how many hours a day the AGV is expected to run.

However, for now, it's unlikely that the AGV will have to work non-stop for a full 8 hour day, and the 6 hour run time is likely sufficient.

4.3.4 3D sketch of the AGV

Having in mind all of the previous considerations, a 3D sketch of the AGV was made to get a better idea of what the real dimensions of the AGV would resemble. The result can be seen in Figures 4.22a and 4.22b. A more detailed view of the AGV and its structure can be seen in Appendix B.

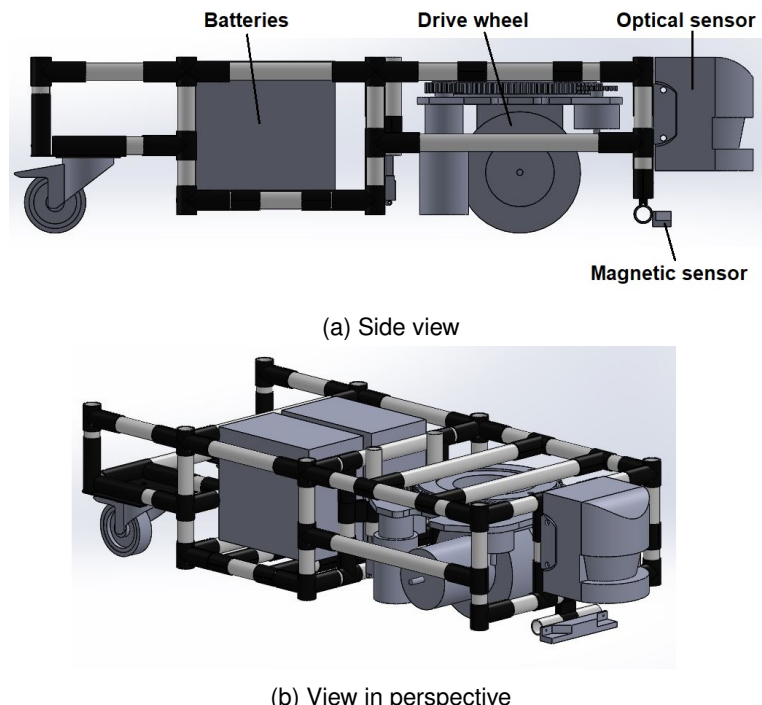


Figure 4.22: 3D drawings of the AGV

4.3.5 Second Design Iteration

Having accomplished a design for the AGV allows for new values that were previously assumed to be corrected.

For starters, the weight of the AGV. For the first iteration, a weight of 75 kg was considered, of which 52 kg constituted the main components. Since for the design the batteries considered were changed, the weight of the components should now amount to 65.15 kg. Taking into account the structure of the AGV is made of steel, and considering a typical value of 7900 kg/m^3 for the density of steel, SolidWorks calculated that the weight of the structure would be of approximately 25 kg. Adding an extra 2 kg to account for the back wheels (including the fork of the wheel) amounts to a total weight of 92.15 kg.

Using SolidWorks, it was also possible to determine the position of the center of mass of the structure. Figure 4.23 shows the weight distribution on the AGV (distances in millimetres).

With this information, and knowing the dimensions of the AGV and the relative position of the main

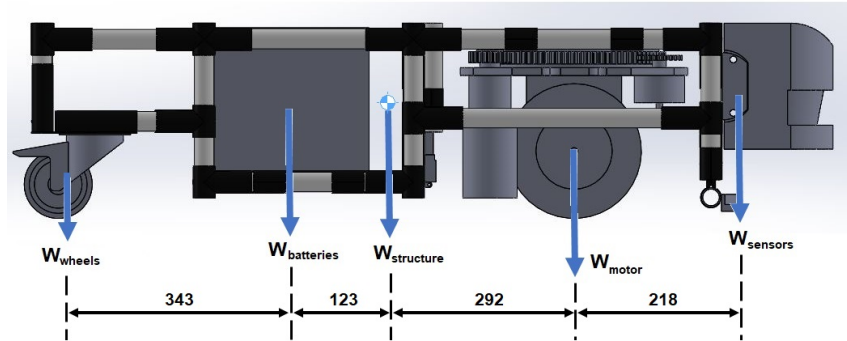


Figure 4.23: Weight distribution on AGV

components, it was possible to determine the position of the AGV's center of mass and determine a new value for L_x .

$$L_x = \frac{25(0.292) + 2 \times 9.8(0.292 + 0.123) + 2 \times 1(0.292 + 0.123 + 0.343) - (3.3 + 0.25)(0.218)}{25 + 2 \times 9.8 + 2 \times 1 + (3.3 + 0.25) + 42} = 0.176 \text{ m} \quad (4.16)$$

Figure 4.23 also provides a new value for l of 0.758 m, and L_y was also measured to be approximately 0.32 m. Table 4.5 shows the new results obtained using the new values.

Table 4.5: Second iteration results

R_4 (N)	$\mu_{rr,4}$	F_4 (N)	F_3 (N)	R_2 (N)	R_1 (N)	$\mu_{rr,2}$	F_2 (N)	F_1 (N)
264.87	0.033	8.99	143.96	135.34	633.31	0.027	3.90	243.91

Applying equation 2.11, once again, results in a new value for the necessary torque.

$$T = F_1 r + I \frac{a}{r} = 243.91 \times (0.198/2) + \left[\frac{1}{2} \times 5 \times (0.198/2)^2 \right] \times \frac{1}{0.198/2} = 24.39 \text{ N} \cdot \text{m} \quad (4.17)$$

This brings down the safety factor from the previously calculated 1.3 to 1.2. However, it's worth to note that the safety factor is being calculated in relation to the torque the motor can provide continuously, since, as seen in Table 4.3, the motor can output a maximum of 180 Nm before stalling. Besides, with a maximum speed of 1.4 m/s and an acceleration of 1 m/s², the AGV isn't expected to have to accelerate for more than 1.4 seconds at a time, so even if at times the output torque surpasses the 29.5 Nm the motor is quoted for, this shouldn't pose a problem to the motor.

Traction of the Motorized Wheel

While the motor may be powerful enough to provide the necessary torque, it's important to check if the motorized wheel has enough traction to the floor, so that it doesn't slip when it begins to roll. Slippage between two materials happens when the force used to drag an object through another exceeds the

maximum static friction force, given by equation 4.18, where μ_s is the static friction coefficient between those two materials and R is the normal reaction.

$$F_{sf} = \mu_s R \quad (4.18)$$

In this case, the normal reaction is the last calculated R_1 , which is of 633.31 N. The floor on the workshop is concrete and the material of the tyre of the wheel is polyurethane. According to Beer et al. [7], the coefficient for static friction between rubber and dry concrete can vary between 0.6 to 0.9. Polyurethane can in some cases be used as a replacement for rubber, since polyurethane is a material that can outperform rubber in many ways (refer to Table 4.6). However, due to rubber typically being softer than polyurethane, it usually also provides better traction.

Table 4.6: Attributes of Polyurethane and Rubber [36]

	Rubber	Polyurethane
Load Capacity	Good	Excellent
Tear Resistance	Fair	Excellent
Abrasion Resistance	Fair	Excellent
Traction	Excellent	Good
Cushioning	Excellent	Fair
Rolling Resistance	Good	Excellent
Floor Marking	Fair	Excellent
High Speed Operation	Excellent	Good
Outside operation	Excellent	Fair
Inside operation	Good	Excellent
Wet Floors	Excellent	Good

A value of $\mu_s = 0.6$ between polyurethane and concrete was assumed, so as to be comparable to a harder rubber. This results in a maximum static friction force of 380 N. Since this value is bigger than the 243.91 N calculated for the tractive effort, it can thus be concluded that the wheel will not slip.

Calculations for worst case scenarios

Calculations were performed to determine what would happen in the case the wheels of the cart would, for whatever reason, jam and stop rolling, and instead the AGV would have to drag the cart. For these calculations, the kinetic friction coefficient was used instead, which, according to Beer et al. [7], tend to be approximately 25% smaller than the static friction coefficient. Since the tyres of the cart are made of rubber, a value of $\mu_k = 0.68$ (75% of $\mu_s = 0.9$) was considered. It was also calculated whether the motorized wheel would slip or not in these conditions and how the AGV would have to adjust its acceleration in order for the wheel not to slip. The results can be seen in Table 4.7.

Table 4.7: Jammed wheels with cart in movement

# of jammed wheels	Tractive effort	Torque	Max. Static Friction	Slip condition	Adjusted acceleration
1	417.6 N	41.6 Nm	336.6 N	Yes	0.65 m/s ²
2	591.5 N	58.8 Nm	293.3 N	Yes	-0.29 m/s ²
3	765.7 N	76.1 Nm	250.0 N	Yes	-1.24 m/s ²
4	940.0 N	93.3 Nm	206.6 N	Yes	-2.19 m/s ²

The conclusion that can be taken from these results is that, while the motor would be powerful enough to not stall in any of these conditions, the AGV could only potentially not be affected by the situation if only one of the cart's wheels were to stop rolling while already in motion. In that scenario, the AGV would have to be moving at constant speed or with a maximum acceleration of 0.65 m/s^2 .

The same calculations can be performed assuming now the situation where the AGV is trying to pull the cart from a resting state. This would mean the motor would have to overcome a static friction force ($\mu_s = 0.9$) instead of a kinetic one. The results can be seen in Table 4.8

Table 4.8: Jammed wheels with cart in resting state

# of jammed wheels	Tractive effort	Torque	Max. Static Friction	Slip condition	Adjusted acceleration
1	476.8 N	47.4 Nm	321.9 N	Yes	0.32 m/s^2
2	710.1 N	70.6 Nm	263.8 N	Yes	-0.94 m/s^2
3	943.8 N	93.7 Nm	205.7 N	Yes	-2.21 m/s^2
4	1177.6 N	116.8 Nm	147.6 N	Yes	-3.50 m/s^2

Similar conclusions can be taken from the first case, while the motor would not stall in any of the conditions, the motorized wheel would always slip, except in the case of only one jammed wheel, in which case the AGV would only be able to pull the cart at a maximum acceleration of 0.32 m/s^2 .

4.3.6 Further design considerations

Charging systems

There are two types of charging systems that are usually used in AGVs: contact and contactless charging systems.

The contact charging systems typically consist in a base plate connected to a battery charger, and can be installed on the floor or on a lateral support by the side of the AGV's path, and a current collector, which is typically installed at the bottom or on the side of the AGV. They work by simply providing electrical contact between the battery terminals and the charger once the collector and the base plate come into physical contact. Figure 4.24 shows an example of a system of this type by the company Vahle.



Figure 4.24: Contact charging system [37]

This kind of solution has the advantage of being very straightforward and simple in terms of its functionality and installation, its main disadvantage being the fact that the continuous contact might lead

to the wear of the parts due to friction. If placed on the floor, it can also be affected by dirt.

Contactless charging systems, on the other hand, charge the batteries through electromagnetic induction. They consist usually in two plates, one of them being connected to a power transferring unit (primary plate) and the other to a power receiving unit (secondary plate). The system is placed similarly to the contact charging systems, with the primary plate being on the floor or on a lateral support, and the secondary plate being on the bottom or the side of the AGV. Each plate contains a coil. The primary coil is connected to an AC power source, which leads to an alternating current being passed through the coil, generating an alternating magnetic field. When the secondary coil comes into contact with the magnetic field it converts it back into electric current, charging the battery [38]. Figure 4.25 shows a schematic of a product by company Delta Energy Systems.

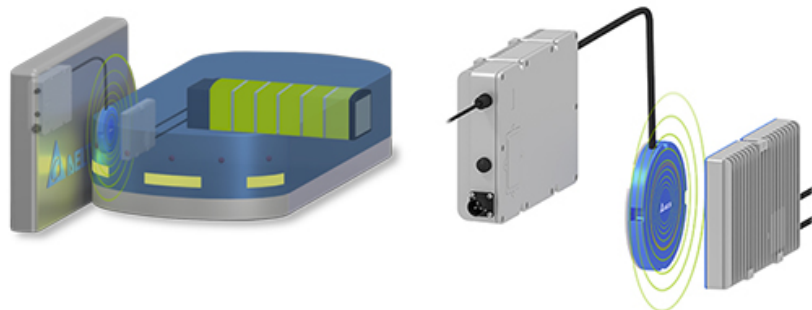


Figure 4.25: Contactless charging system [39]

Since in order for the battery to be charged, the secondary coil only needs to come into contact with the magnetic field generated by the primary coil, there is no need for them to come into physical contact, thus making it a contactless system. This is an advantage when comparing to contact charging systems, since there will be no wear of the parts due to friction. Its disadvantages include the fact they tend to be less efficient than a contact system solution [40], and the efficiency can go down even further if there is misalignment between the coils.

From a general perspective, both solutions could be adequate for this project. However, the final decision would require a more in depth market study and a better knowledge on how each would impact the performance of the AGV.

Chapter 5

Structural Analysis

Having the design been made and the loads involved analysed and calculated, it is now necessary to make sure that the structure of the AGV can withstand such loads. For that, it is necessary to determine the mechanical properties of the material and use that to do a finite element analysis (FEA). There are many commercially available software that can perform FEA, but for this project the one used was Siemens NX, mainly because it was the one the author had more experience with and was more comfortable using.

5.1 Material Properties

As has been mentioned throughout this thesis, the material used to design both the cart and the AGV is comprised of steel tubes connected by steel joints. The tubes have a 28.6 mm outer diameter and have a thermoplastic coating. The coating has a 0.8 mm thickness, and covers a steel tube of 27 mm outer diameter, which can have 1 mm (T1) or 2 mm (T2) thickness, as can be seen in Figures 5.1a and 5.1b.

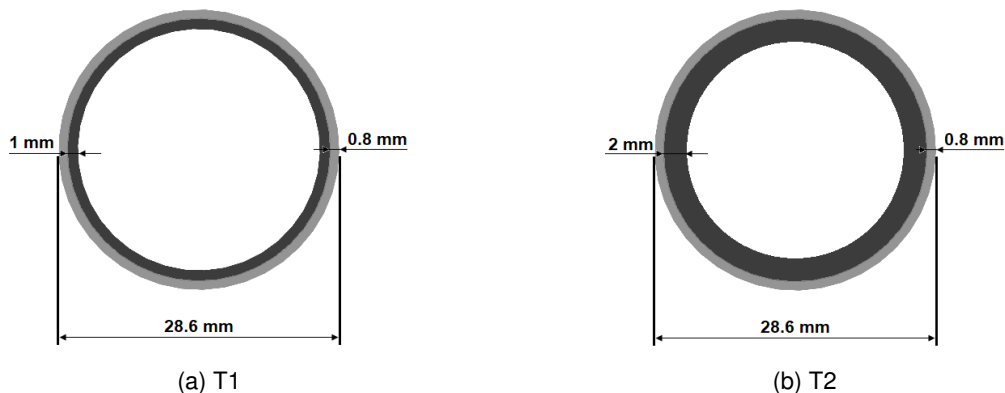


Figure 5.1: Tube sections (lighter grey represents the coating while the darker grey represents the steel)

The company provided the information that the steel was a E260 type steel, but didn't provide the specific properties of this material. However, their catalogue [41] contains tables which display experimental results for tubes suspending a central load (refer to Figure 5.2), done with different loads (P) and

with variable distancing between supports (L). The values can be seen in Tables 5.1 and 5.2 and all the values were taken in elastic regime.

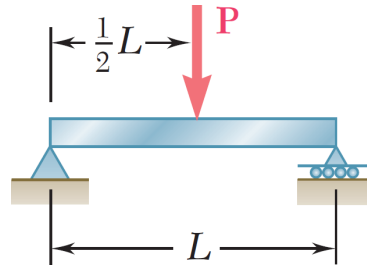


Figure 5.2: Simply supported beam with central load [42]

Table 5.1: Deflection in mm for a T1 tube suspending a central load

Suspended load (kg)	Distance between supports (m)							
	0.75	1.00	1.25	1.50	1.75	2.00	2.25	2.50
10	0.87	2.09	4.00	6.95	10.95	16.19	23.80	32.38
25	2.19	5.14	10.0	17.14	27.62	40.95	58.09	80.0
50	4.28	10.28	20.0	34.28				
75	6.47							

Table 5.2: Deflection in mm for a T2 tube suspending a central load

Suspended load (kg)	Distance between supports (m)							
	0.75	1.00	1.25	1.50	1.75	2.00	2.25	2.50
10	0.48	1.14	2.28	3.90	6.19	9.14	13.33	18.09
25	1.24	2.85	5.62	9.71	15.23	22.85	32.38	44.76
50	2.38	5.71	11.24	19.04	30.47	45.71	65.71	89.52
75	3.62	8.57	17.14	28.57	45.71	68.57		
100	4.86	11.43	22.86	39.04				
125	6.09	14.28	28.57					

According to Beer et al. [42], the analytical expression for the maximum deflection of a beam in a loading condition as the one seen in Figure 5.2 is as follows (5.1):

$$y_{max} = \frac{PL^3}{48EJ} \quad (5.1)$$

where E is the Young's modulus of the beam and J is the second moment of area of the cross section. For an annulus of inner radius r_1 and outer radius r_2 , the second moment of area is given by equation (5.2).

$$J = \frac{\pi}{4} (r_2^4 - r_1^4) \quad (5.2)$$

For tube T1, $r_2 = 13.5$ mm and $r_1 = 12.5$ mm result in a second moment of area of $J_1 = 6.91 \times 10^{-9}$ m⁴, and for tube T2, $r_2 = 13.5$ mm and $r_1 = 11.5$ mm give a second moment of area of $J_2 = 1.24 \times 10^{-8}$ m⁴. Note that only the steel part of the tube is being considered, and not the coating, as that is what is carrying the great majority of the loads. Using these results, equation (5.1), and the data from Tables 5.1 and 5.2 it is thus possible to calculate a Young's modulus for each case, and to obtain an average

Young's modulus from those results. Tables 5.3 and 5.4 show the resulting Young's modulus for each case from Tables 5.1 and 5.2, respectively.

Table 5.3: Young's modulus in GPa for T1

Suspended load (kg)	Distance between supports (m)							
	0.75	1.00	1.25	1.50	1.75	2.00	2.25	2.50
10	143.37	141.47	144.37	143.58	144.71	146.10	141.51	142.68
25	142.39	143.81	144.37	145.55	143.43	144.41	144.94	144.37
50	145.72	143.81	144.37	145.55				
75	144.59							

Table 5.4: Young's modulus in GPa for T2

Suspended load (kg)	Distance between supports (m)							
	0.75	1.00	1.25	1.50	1.75	2.00	2.25	2.50
10	145.44	145.16	141.76	143.20	143.28	144.84	141.41	142.93
25	140.75	145.16	143.77	143.79	145.58	144.84	145.53	144.42
50	146.66	144.90	143.77	146.66	145.53	144.81	143.43	144.42
75	144.64	144.82	141.43	146.61	145.52	144.80		
100	143.65	144.78	141.38	143.06				
125	143.29	144.85	141.41					

The average Young's modulus achieved was of 144.1 GPa. This, however, is not compatible with typical values for the modulus of elasticity of steel, which usually fall between 190 – 200 GPa [42]. From an engineering perspective it makes no sense to use a value that clearly doesn't match the description of the material being used and, unfortunately, due to time constraints, it was not possible to recreate the tests to corroborate or correct the deflection values that the company provides. As such, the decision was made to use typical values for this type of steel provided by an online material properties database [41], which can be seen in Table 5.5.

Table 5.5: Mechanical properties for E260 steel

Young's Modulus (GPa)	Poisson's Ratio	Yield Strength (MPa)
190	0.29	290

As for the joints, the TechnoLean catalogue [41] states that they can endure a load of 100 kg being applied to a tube axially or transversally before the joint is separated from the tube or slides across one.

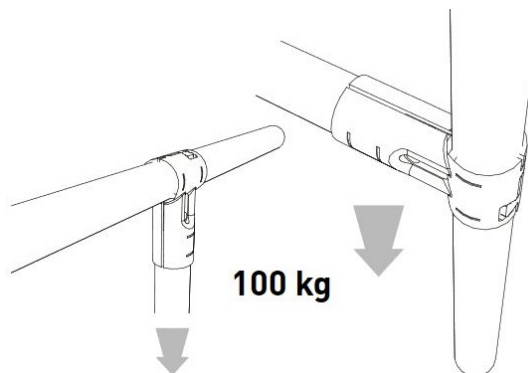


Figure 5.3: Joint strength (Adapted from [41])

5.2 Finite Element Analysis

5.2.1 Finite Element Method

There are typically three approaches that can be taken when trying to solve an engineering problem:

- **The analytical method**, which bases on a series of assumptions and simplifications regarding the physics of the problem to reach a general equation that described that problem. It is usually best for simpler problems.
- **The experimental method**, which consists in recreating the problem and directly measuring the results. It's important to note that this is the only method that provides real results and not approximations.
- **The numerical method**, which convert differential equations that characterize a continuum into algebraic equations that describe a discreet model of that continuum [43].

The finite element method (FEM) is a numerical method. Numerical methods are typically used when a problem becomes too complicated to be solved by analytical methods, whether it be due to complicated geometries, complex material constitution, or nonlinearities. They are widely used in simulation computer programs for design applications, since it facilitates the study of the effects of different parameters on the system without the need for a variety of experimental testing, making it time saving and cost effective. The basic idea behind the finite element method is that it takes a given geometry and divides it into smaller pieces, called finite elements, over each of which an algebraic equation that is compatible with the neighbouring elements is derived. These equations are then solved simultaneously to obtain the solution to the problem as a whole. [43]

5.2.2 Meshing

As was explained before, to apply the FEM the geometry must be divided into elements. These elements connect to each other through nodes. Together, the elements and the nodes form a mesh in the shape of the initial geometry. Creating the mesh is a pivotal step of the FEA, as the quality of the results generated correlates directly with the quality of the mesh [44]. However, the more refined a mesh is, the more computational effort it will require to solve the problem, which can lead to high computation time.

The first step in meshing is selecting the type (or types) of elements that are going to be used for the analysis. This decision should be made based on the geometry of the structure, but also on the type of analysis and time allotted to the project. [44] There are three main types of elements:

- **1D elements** are typically used when one dimension is much larger than the other two (e.g. rods, beams, pipes).
- **2D elements** are typically used when two of the dimensions are very large in comparison to the third one (e.g. thin sheet metal parts).

- **3D elements** are typically used when all three dimensions are comparable in size.

Because the structure is composed of tubes, 1D elements were deemed appropriate for this analysis, and, since they have constant section and material, CBAR elements were chosen, since they allow tension, compression, and bending stresses [45].

To simulate contact between some tubes, RBE2 elements were used, which is a type of element that works as a rigid link to transfer displacements from an independent node to other dependant nodes.

5.2.3 Modelling the geometry

When modelling a geometry with 1D elements, its shape is attributed by the characteristics of the mesh, and the geometry needs to be represented solely by lines representing the centre of the cross section, as can be seen in Figure 5.4a. For the analysis, all the tubes were defined as T1 tubes, the purpose being to check if there were any tubes that needed reinforcement and required to be replaced by thicker tubes, while the pins were modelled as cylinders with a 12.3 mm radius. The meshed geometry can be seen in Figure 5.4b.

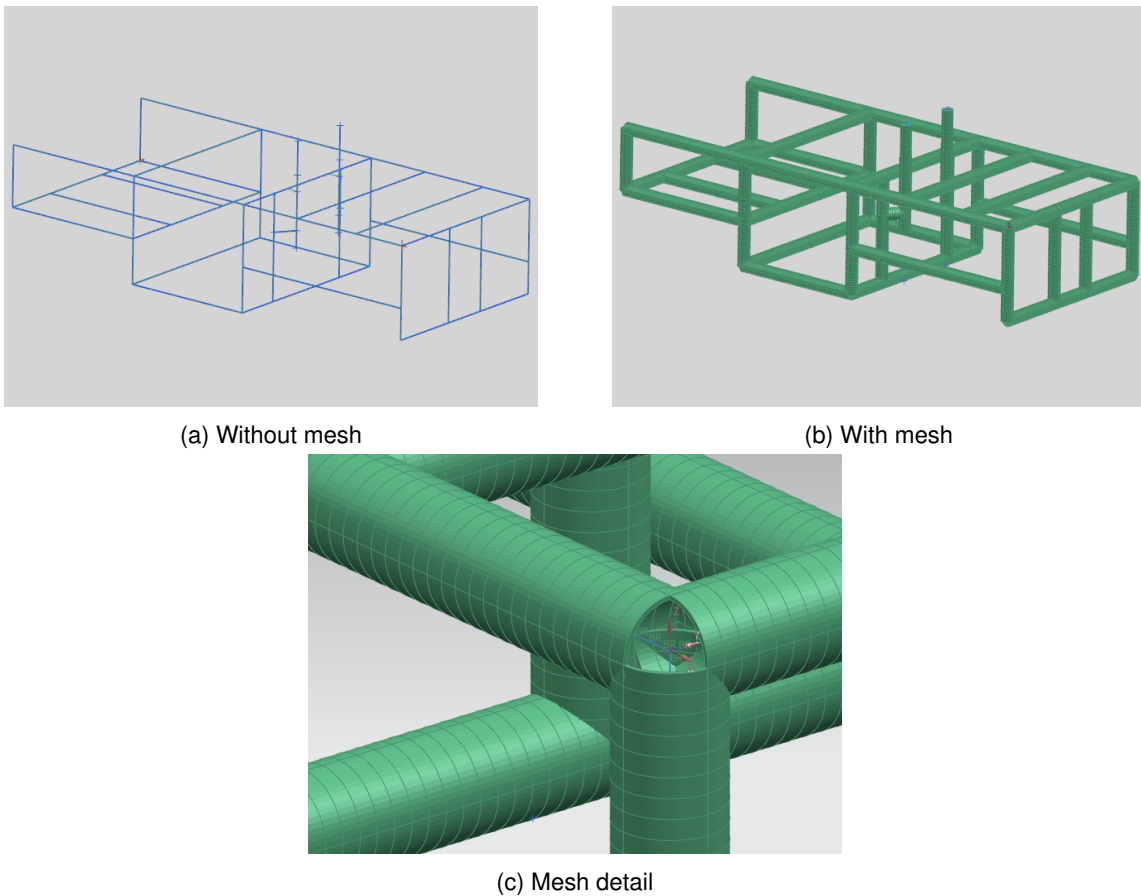


Figure 5.4: Modelling of the AGV

The joints that connect the tubes, however, were not modelled, and instead the tubes were connected directly at the corners by making adjustments on the length of the tubes to still convey the real dimensions of the structure. This strays a little bit from reality and will likely portray the joints as more

flexible than they should actually be and induce some error in the results of the simulation, but since the joints are also made of steel and somewhat work as an extension of the tubes, the results should still be in the same order of magnitude than the real results.

5.2.4 Loads and Constraints

The loads, which can be seen represented in red in Figure 5.5b, were applied so as to represent the weight of the structure itself, as well as the weight of the components of the AGV, and the force representing the pulling of the cart. The weights of the wheels were not represented seeing as the structure will be supported by them, and not exactly be under the effect of their weight. Instead, the wheels were represented by the constraints, represented in orange in Figure 5.5a. The way the constraints were represented were that, for the motorized wheel, the structure was fixed in four points at approximately the positions where the drive wheel would be bolted to the tubes, and the back wheels were represented by two simply supported constraints.

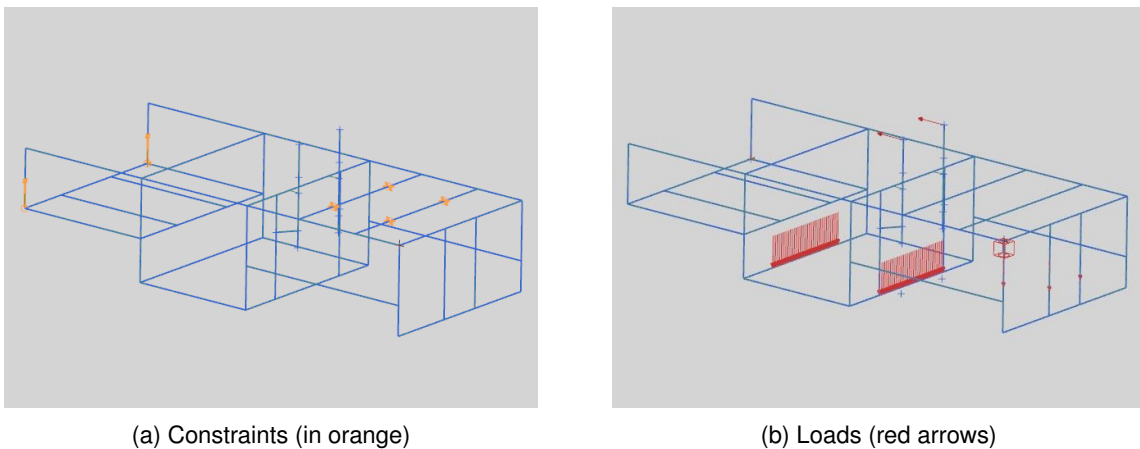


Figure 5.5: Loads and constraints

5.2.5 Linear Static Analysis

A linear static analysis was then performed. A linear static analysis is one where the material follows a linear elastic behaviour and the forces aren't varying with time, and small displacements are assumed [44]. This analysis outputs the stress state and displacements of the structure for the prescribed loading and constraints. In this case, the results will be used to understand if the material will yield by comparing the stresses with the yield strength of the material, and check for reasonable deformation.

It's worth to notice that this analysis isn't perfectly representative of the typical behaviour of the AGV, seeing as it required the structure to be constrained in a way that doesn't represent the motion of the AGV. Still, this analysis will allow for a general idea of how the structure will behave, and as it should lead to bigger stresses than those that would develop in real life, it will err on the side of safety.

Mesh Convergence

As mentioned before, a quality mesh leads to quality results, but an overly refined mesh isn't necessarily better than one that is less refined. In reality, as a mesh is increasingly refined, what can be observed is that the results eventually converge to a plateau of acceptable accuracy, where the results don't really yield significant differences.

A mesh convergence study was thus performed. The results for the von Mises stresses were recorded for tests with element lengths of 80 mm, 60 mm, 40 mm, 30 mm, 20 mm, 10 mm, 5 mm, 2.5 mm, and 1 mm. As can be seen in Figure 5.6, convergence was achieved at 5 mm. The tests were done using the maximum value of von Mises stresses because that is the value that is going to be compared to the yield strength of the material to verify if the material suffers plastic deformation or not.

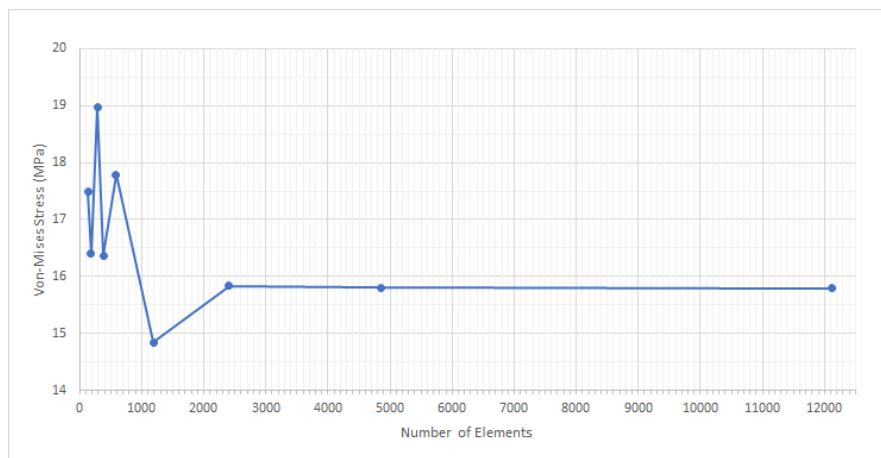


Figure 5.6: Mesh convergence study

Results and Conclusions

The results obtained from the finite elements analysis where the total displacements, the maximum von Mises stress, the shear forces in the Y and Z directions of the local referential of each element, and the axial forces. The results can be seen in Table 5.6 and in Figures 5.7 to 5.11.

Table 5.6: FEA results

	Displacement	von Mises	Shear Force XY	Shear Force XZ	Axial Force
Minimum	0 mm	0 MPa	-135.12 N	-71.52 N	-59.01 N
Maximum	0.177 mm	15.81 MPa	135.38 N	73.68 N	77.72 N

The displacements give us a general idea of how much the structure will deform when under these loads. The maximum displacement is of 0.177 mm, meaning the structure will barely deform.

As for the von Mises stresses, these relate to the von Mises yield criterion, which states that a material will start yielding (i.e. suffering irreversible deformations) when the von Mises stresses reach the value of the yield strength of that material. Previously, it was established that the yield strength of the steel of the tubes is of 290 MPa (refer to Table 5.5). The analysis showed that the maximum von

Mises stress reached was of 15.81 MPa, meaning the loads are not likely to cause the structure of the AGV to yield.

The shear forces and the axial force can be compared to the joint strength given by the company, which was of 100 kg, which is approximately 981 N. That value is as well much superior than any of the values the analysis registered, meaning there is also very little risk of the joints separating or sliding.

The overall conclusion from this analysis is that the designed structure is safe from deformation and from dismantling.

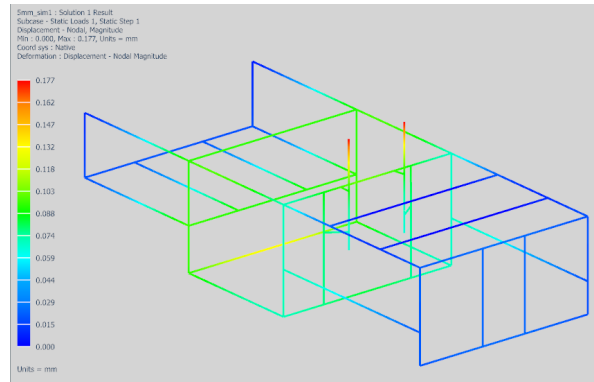


Figure 5.7: Displacement – Magnitude

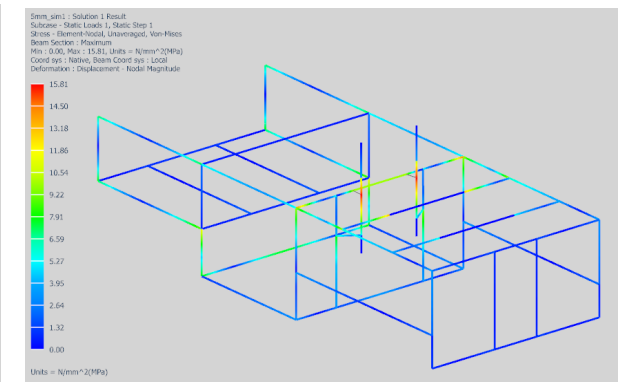


Figure 5.8: von Mises Stress

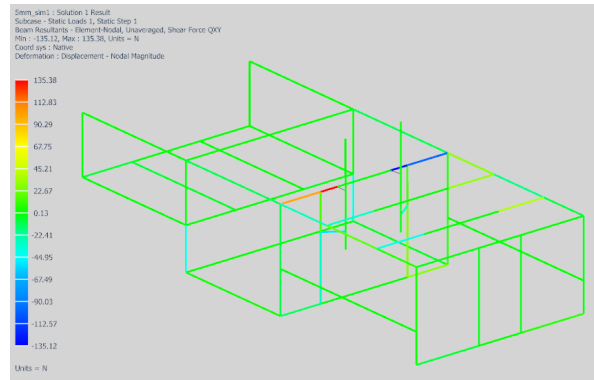


Figure 5.9: Shear Force XY

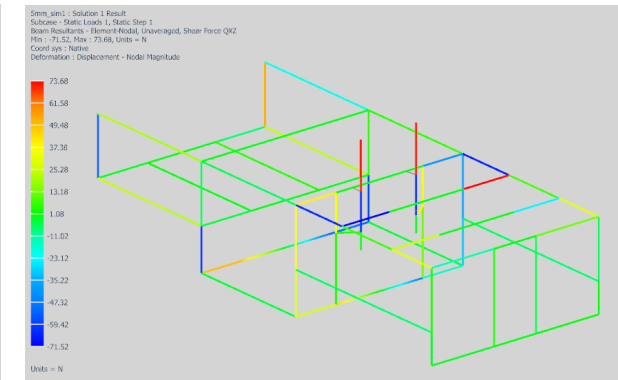


Figure 5.10: Shear Force XZ

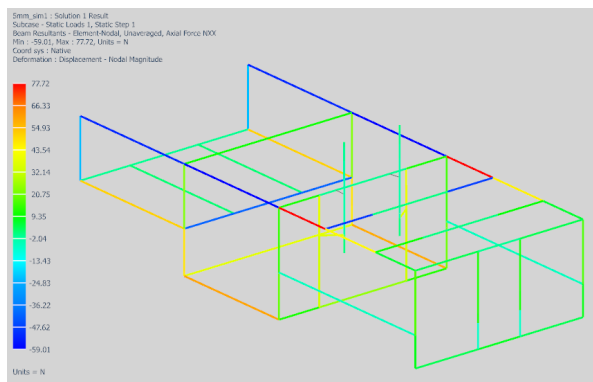


Figure 5.11: Axial Force

Chapter 6

Conclusions

In this thesis, a functional concept for the material distribution mechanism was achieved, as well as a design for the AGV.

It was concluded that the current carts used at the workshop need adaptations in order to be made compatible with an AGV, but those adaptations are very minor and should not impact the structural soundness of the cart when it comes to carrying material. For this reason, a structural analysis was not performed on the cart. However, it was also concluded that some of the stations, namely the expedition stations, need to be made compatible with the cart, should the suggested alterations be made.

Adaptations were made in regards to the preliminary design of the AGV, namely in the material to be used as well as the type of AGV to be designed. Calculations were performed to determine the loads to which the structure would be subjected to, and two iterations were performed to achieve the final results. It was also possible to conclude that the AGV should have enough traction to the floor of the workshop in order to be able to pull a fully loaded cart without slipping, but that the same will not be achieved if more than one of the cart's wheels should stop spinning.

As for the structural analysis, it was not possible to achieve compatibility between the experimental results provided by the company that supplies the material and the materials' properties, which raises questions on whether the experimental results should be revised. However, time constraints did not allow for performing these experiments. Using typical values, the FEA showed that the structure of the AGV should withstand the loads it will be subjected to without yielding and without causing separation of joints.

6.1 Future Work

Since the main focus of this thesis was on the structural and mechanical design of the AGV and the delivery system, a lot is yet to be said about the robotic aspect of it. Seeing as the AGV is, at its core, a robot, it's really its electronic composition that is at the heart of its performance.

It is thus paramount that a further study be made into the electronic components that would be required and adequate to be used on this project, as well its circuit design, and also the construction of

a prototype. It is also necessary to create an algorithm for the operation and do the programming and control of the AGV, and to create a user friendly platform to be used by the workers at the workshop to instruct the AGV, and create schedules and routes for it.

It would also be advisable to look into the usage of sensors on the carts and/or on the reception and expedition stations to be used as extra safety measures and ensure the correct delivery of trays.

Bibliography

- [1] G. Ullrich. *Automated Guided Vehicle Systems: A Primer with Practical Applications*. Springer-Verlag Berlin Heidelberg, 1st edition, 2015. ISBN 978-3-662-44813-7.
- [2] Business Insider. Amazon now has 45,000 robots in its warehouses. URL <https://www.businessinsider.com/amazons-robot-army-has-grown-by-50-2017-1>. Accessed: 02-05-2019,
- .
- [3] Conveyco. The Advantages and Disadvantages of Automated Guided Vehicles (AGVs). URL <https://www.conveyco.com/advantages-disadvantages-automated-guided-vehicles-agvs/>. Accessed: 02-05-2019, .
- [4] C. Feledy and M. S. Luttenberger. A State of the Art Map of the AGVS Technology and a Guideline for How and Where to Use It. Master's thesis, Lund University, 2017.
- [5] E. S. Martínez. Preliminary Design of an Automated Guided Vehicle (AGV) System. Master's thesis, Instituto Superior Técnico, 2018.
- [6] J. Larminie and J. Lowry. *Electric Vehicle Technology Explained*. John Wiley & Sons Ltd, 1st edition, 2003. ISBN 0-470-85163-5.
- [7] F. P. Beer, E. R. Johnston, D. F. Mazurek, and P. J. Cornwell. *Vector Mechanics for Engineers: Statics and Dynamincs*. McGraw-Hill, 10th edition, 2013. ISBN 978-0-07-339813-6.
- [8] Elesa Ganter. Castors and Wheels. URL https://www.elesa-ganter.com/static/technicaldata/files/Castors_and_Wheels_TD_EN.pdf. Accessed: 01-04-2019, .
- [9] F. M. White. *Fluid Mechanics*. McGraw-Hill, 4th edition, 2001. ISBN 978-0-07-069716-4.
- [10] H. Rouse. *Elementary Mechanics of Fluids*. Dover Publications, 1946. ISBN 0-486-63699-2.
- [11] R. A. Serway and J. W. Jewett. *Physics for Scientists and Engineers*. Thomson Brooks/Cole, 6th edition, 2004. ISBN 0534408427.
- [12] Kaizen Institute. O que é Kaizen? URL <https://pt kaizen com quem-somos/significado-de-kaizen html>. Accessed: 16-04-2019, .
- [13] M. Imai. *Kaizen: The Key To Japan's Competitive Success*. McGraw-Hill, 1986. ISBN 978-0-07-554332-9.

- [14] Kaizen Institute. What is the difference between Kaizen, Lean & Six Sigma? URL <https://in.kaizen.com/blog/post/2015/09/11/what-is-the-difference-between-kaizen-lean--six-sigma.html>. Accessed: 16-04-2019, .
- [15] Kaizen Institute. Glossary. URL <https://www.kaizen.com/learn-kaizen/glossary.html>. Accessed: 16-04-2019, .
- [16] Lean Enterprise Institute. What is Lean. URL <https://www.lean.org/WhatsLean/>. Accessed: 16-04-2019, .
- [17] ROBOEQ. Mgs1600gy. URL <https://www.roboteq.com/index.php/component/virtuemart/320/mgs1600cgy-magnetic-sensor-with-gyroscope-detail?Itemid=972>. Accessed: 05-04-2019, .
- [18] Medica Magazine. Custom Upgrade and Refurbishment. URL https://www.medica-tradefair.com/cgi-bin/md_medica/lib/pub/tt.cgi/Custom_Upgrade_and_Refurbishment.html?oid=26492&lang=2&ticket=g_u_e_s_t. Accessed: 11-02-2019, .
- [19] HYMO. Axx4-8/6 P. URL <https://hymo.com/product/axx4-86p/>. Accessed: 05-04-2019.
- [20] ROBOEQ. Building a Magnetic Track Guided AGV. URL <https://www.roboteq.com/index.php/applications/100-how-to/278-building-a-magnetic-track-guided-agv>. Accessed: 11-02-2019, .
- [21] C.F.R. Horizzont Drive Wheels. URL <http://www.cfritaly.com/elencoprodotti.php?idc=7>. Accessed: 04-04-2019.
- [22] Technolean. Connectors. URL <https://www.technolean.com/en/category-product/connectors>. Accessed: 15-04-2019.
- [23] All About Lean. Fundamentals of Karakuri Kaizen. URL <https://www.allaboutlean.com/karakuri-fundamentals/>. Accessed: 15-04-2019, .
- [24] C. Chabiron. Here is the proof that kaizen leads to real innovation. URL <https://planet-lean.com/karakuri-kaizen-aio-lean-transformation/>. Accessed: 15-04-2019.
- [25] All About Lean. Introduction to Karakuri Kaizen. URL <https://www.allaboutlean.com/karakuri-introduction/>. Accessed: 15-04-2019, .
- [26] item. Karakuri. URL <http://karakuri.item24.de/en/>. Accessed: 16-04-2019, .
- [27] item. Benefits of Karakuri. URL <http://karakuri.item24.de/en/benefits.html>. Accessed: 16-04-2019, .
- [28] item. Release Unit D30 Bar T1. URL <https://product.item24.de/en/products/product-catalogue/productdetails/products/low-cost-automation-the-mechanical-solution-1001390644/release-unit-d30-bar-t1-65884/>. Accessed: 15-04-2019, .

- [29] Technolean. TR-400. URL <https://www.technolean.com/en/articles/roller-tracks-and-accesories/tr-400/>. Accessed: 16-04-2019, .
- [30] T. P. Ferreira and I. A. Gorlach. Development of an affordable automated guided cart for material handling tasks. *International Journal of Circuits and Electronics*, 1, 2016. ISSN: 2367-8879.
- [31] Technolean. TF-125. URL <https://www.technolean.com/en/articles/castors-feet-and-accessories/tf-125/>. Accessed: 16-04-2019, .
- [32] R. V. Levine and A. Norenzayan. The pace of life in 31 countries. *Journal of Cross-Cultural Psychology*, 30(2):178–205, March 1999.
- [33] I. Evans. The rolling resistance of a wheel with a solid rubber tyre. *British Journal of Applied Physics*, 5(5):187–188, March 1954.
- [34] The Engineering Toolbox. Rolling Resistance. URL https://www.engineeringtoolbox.com/rolling-friction-resistance-d_1303.html. Accessed: 9-03-2019, .
- [35] *Materials Data Book*. Cambridge University Engineering Department, 2003.
- [36] Thombert. Polyurethane and Rubber Tires: A Comparative Overview. URL <https://www.thombert.com/userdocs/PolyurethaneRubberTires.pdf>. Accessed: 28-04-2019, .
- [37] Vahle. Charging Contacts. URL <https://www.vahleinc.com/charging-contact-bls-blk-sls.html>. Accessed: 28-04-2019, .
- [38] J. D. de Deus, M. Pimenta, A. Noronha, T. Peña, and P. Brogueira. *Introdução à Física*. McGraw-Hill, 2nd edition, 2000. ISBN 972-733-035-3.
- [39] Delta Energy Systems. Wireless Charging Systems. URL <http://www.deltaenergysystems.com/en/Wireless-Charging-Systems-342.htm>. Accessed: 28-04-2019, .
- [40] G. Bekaroo and A. Seeam. Improving wireless charging energy efficiency of mobile phones: Analysis of key practices. In *2016 IEEE International Conference on Emerging Technologies and Innovative Business Practices for the Transformation of Societies (EmergiTech)*, pages 357–360, Aug 2016.
- [41] Technolean. Components Catalogue. URL https://www.technolean.com/wp-content/uploads/2018/12/181212_Technolean_Catalogo_ENG-web.pdf. Accessed: 30-04-2019, .
- [42] F. P. Beer, E. R. Johnston, D. F. Mazurek, and J. T. DeWolf. *Mechanics of Materials*. McGraw-Hill, 7th edition, 2015. ISBN 978-0-07-339823-5.
- [43] J. N. Reddy. *An Introduction to the Finite Element Method*. McGraw-Hill, 3rd edition, 2006. ISBN 007-124473-5.
- [44] *Practical Aspects of Finite Element Simulation - A Study Guide*. Altair University, 3rd edition, 2015.
- [45] Altair University. 1D Elements. URL https://altairuniversity.com/wp-content/uploads/2017/03/1D_Elements_Extract.pdf. Accessed: 30-04-2019, .

Appendix A

C.F.R. Drive Wheel Technical Datasheet

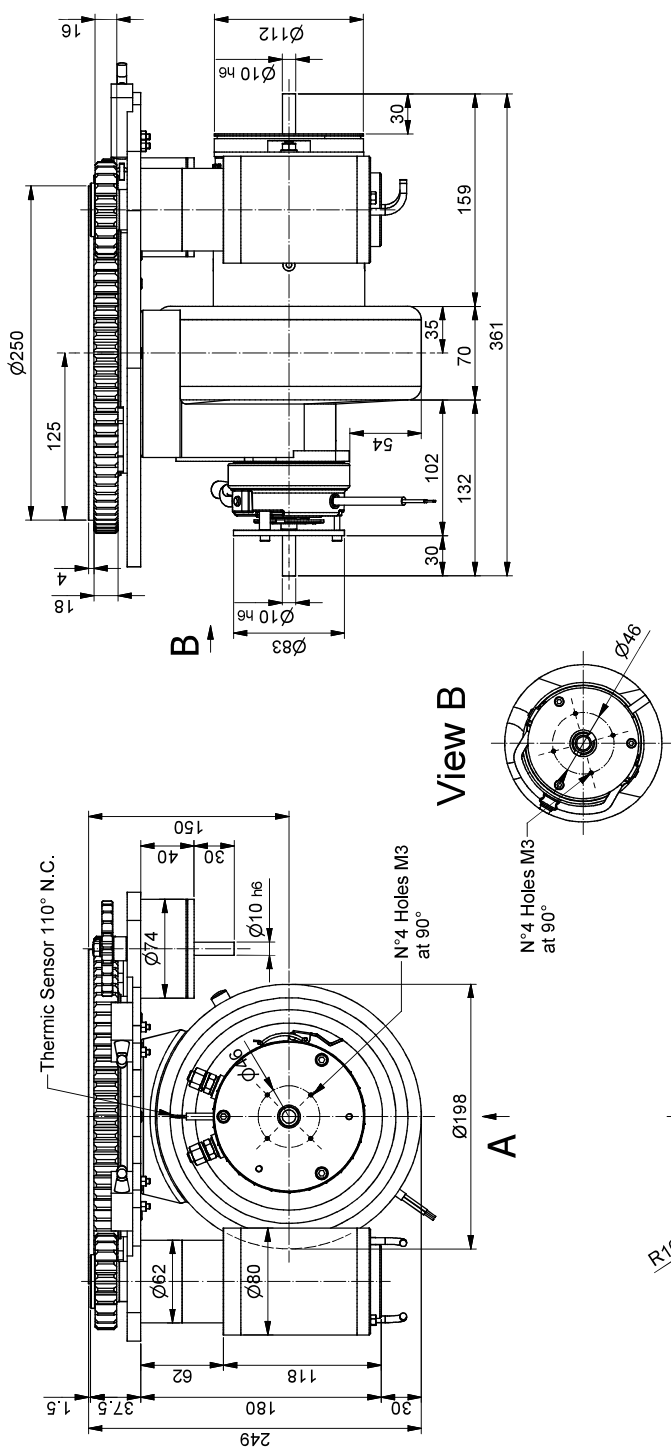
Traction motor data	
Type :	Permanent Magnet Motor
Power (S2 - 60 min)	400 W
Battery voltage	24 V
Speed	2800 Rpm
Current	23 A
Torque	1.36 Nm
Enclosure	IP 20

Traction gear data	
Gear ratio	i 1:30.9
Max accel. and braking torque	Nm 180
Nominal wheel torque	Nm 29.5
Max load on vulkollan wheel	Kg
Max load on polyurethan wheel	Kg 550
Max load on solid rubber wheel	Kg 400
Brake torque	Nm 4
Lubrication	Grease

Steering gearmotor data	
Type	Permanent Magnet Motor
Power (S2 - 60 min)	100 W
Battery voltage	24 V
Motor Speed	3000 Rpm
Current	5 A
Motor torque	0.32 Nm
Gear ratio	i = 1:45.56
Gear Output Torque	Nm = 10.9 Nm
Enclosure	IP 20
Lubrication	Grease

Total Weight Kg 42

Data : Date :	22/12/2016	Scale : Scale :	1 : 4	A3
Dis : Drawn :	M.C.	-		-



Appendix B

AGV Dimensions and Structure

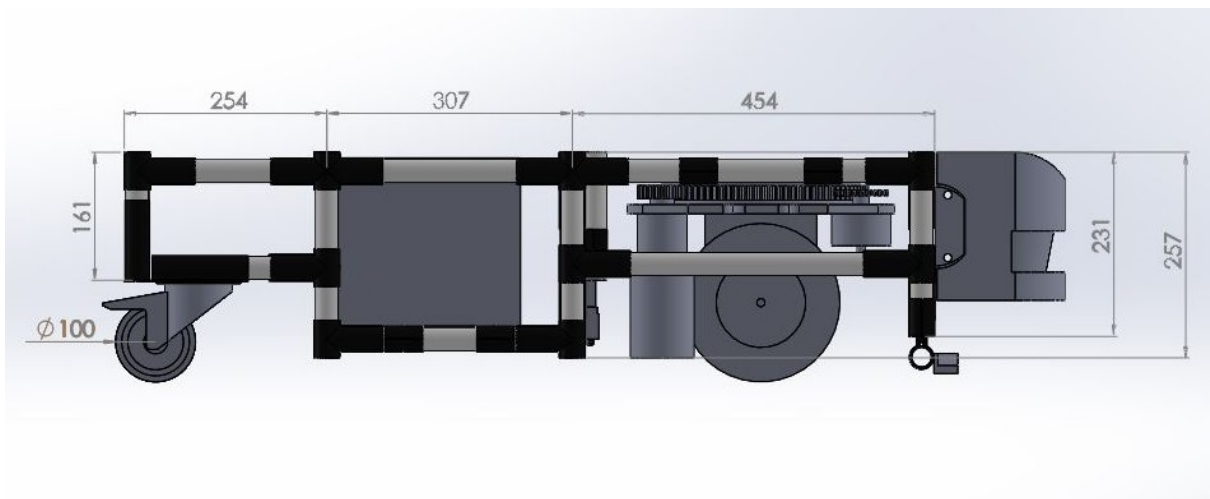


Figure B.1: AGV dimensions, side

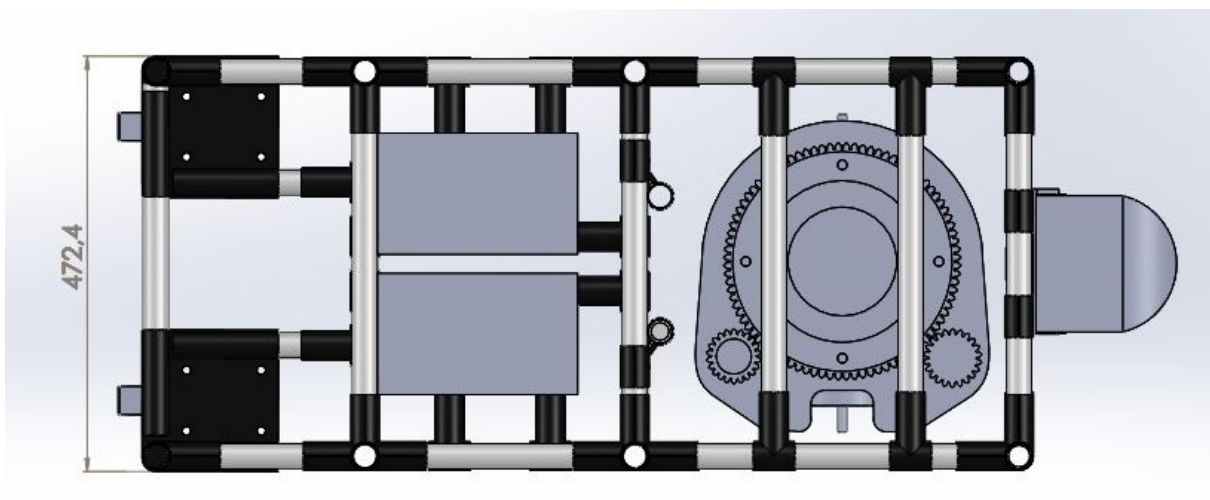


Figure B.2: AGV dimensions, top

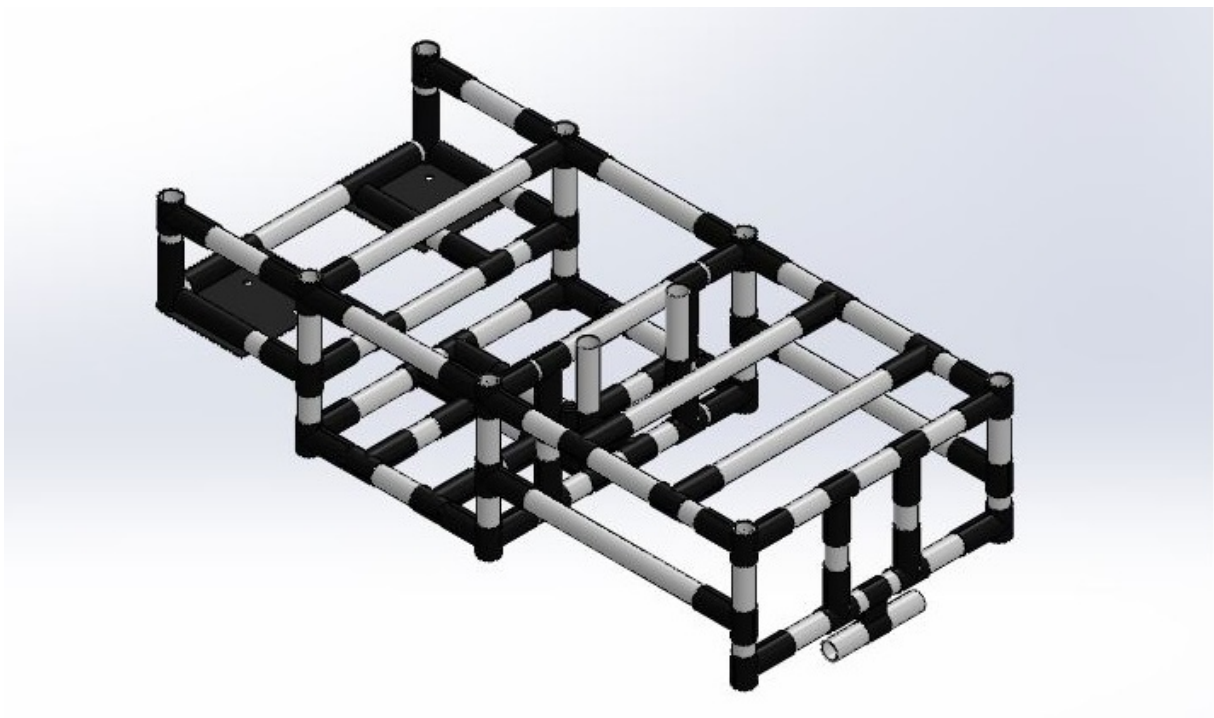


Figure B.3: AGV structure

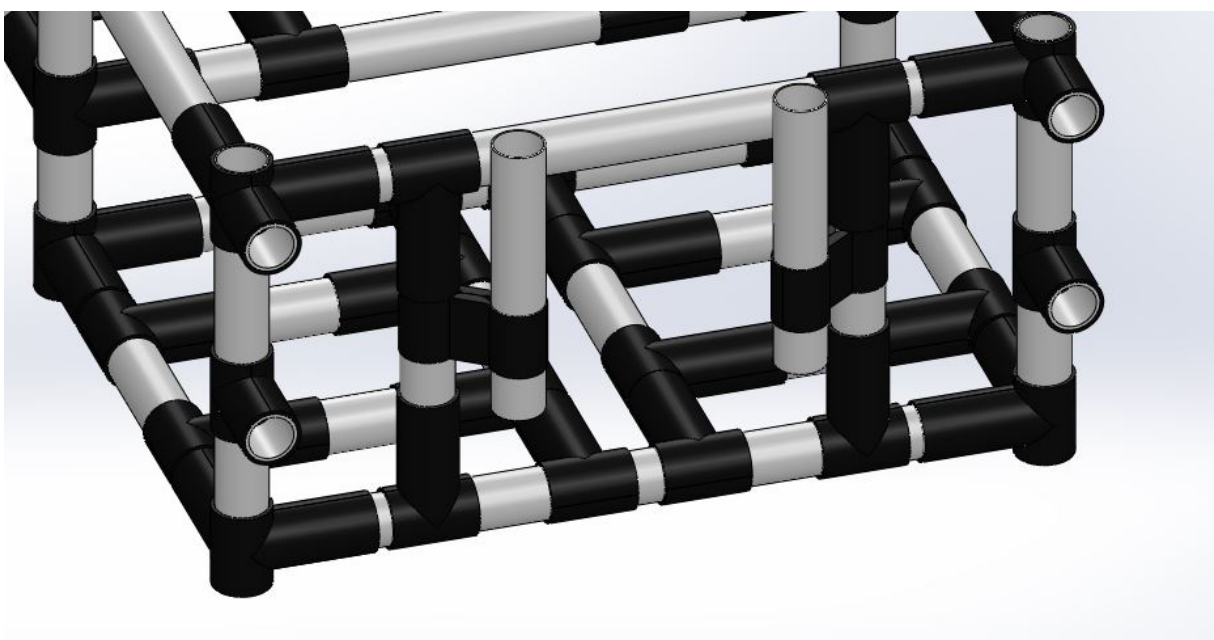


Figure B.4: AGV structure detail